4-23-2014 12:00 AM

The Development and Application of a Forearm Simulator to Investigate Radial Head Biomechanics

Brent A. Lanting
The University of Western Ontario

Supervisor
Graham King
The University of Western Ontario Joint Supervisor
James Johnson
The University of Western Ontario

THE DEVELOPMENT AND APPLICATION OF A FOREARM SIMULATOR TO INVESTIGATE RADIAL HEAD BIOMECHANICS

Thesis format: Integrated Article

by

Brent A. Lanting, BESc, MD, FRCSC

Graduate Program in Medical BioPhysics

Submitted in partial fulfillment
of the requirements for the degree of
Master of Science

The School of Graduate and Postdoctoral Studies
The University of Western Ontario
London, Ontario, Canada

© Brent Lanting, 2013

Abstract

The forearm is a complex articular unit, with poorly understood biomechanics. A novel forearm simulator to facilitate physiologic testing of cadavers for multiple clinical scenarios was designed, manufactured and validated. The simulator had good repeatability and reproducibility. A number of outcome measurements were potentiated including the forearm's resistance to rotation, radiocapitellar contact pressure and area as well as Interosseous Membrane (IOM) loads. Testing of changes to forearm biomechanics due to radial head excision and variations of radial head arthroplasty dimensions was conducted. Radial head arthroplasty using the correct radial head length and diameter recreated the biomechanics of an intact forearm. Radial head excision as well as an implant of non-anatomic length or diameter created abnormal radiocapitellar joint properties and load transfer within the forearm. If radial head arthroplasty is clinically required, an implant that is similar in dimensions to the native radial head maintains native forearm biomechanics.

Keywords

Radial head arthroplasty, over-stuffing, IOM, central band, radiocapitellar contact area, radiocapitellar contact pressure, radial head diameter, load transfer, forearm biomechanics

Co-Author Statement

Chapter 1:   Brent Lanting – Sole Author

Chapter 2:   Brent Lanting – Simulator design, modelling and drawings, supervision of manufacture, data collection and analysis

Louis Ferreira – Simulator design, data collection and analysis

Jim Johnson – Simulator design

Graham King – Simulator design

Chapter 3:   Brent Lanting – Study design, data collection, data analysis, wrote manuscript

Louis Ferreira – Study design, data collection, data analysis, review of manuscript

Jim Johnson – Study design, review of manuscript

George Athwal – Study design, review of manuscript

Graham King – Study design, review of manuscript

Chapter 4:   Brent Lanting – Study design, data collection, data analysis, wrote manuscript

Louis Ferreira – Study design, data collection, data analysis, review of manuscript

Jim Johnson – Study design, review of manuscript

George Athwal – Study design, review of manuscript

Graham King – Study design, review of manuscript

Chapter 5:   Brent Lanting – Study design, data collection, data analysis, wrote manuscript

Louis Ferreira – Study design, data collection, data analysis, review of manuscript

Jim Johnson – Study design, review of manuscript

George Athwal – Study design, review of manuscript

Graham King – Study design, review of manuscript

Chapter 6:   Brent Lanting – Sole author

Acknowledgments

There are so many people to thank for their efforts and contributions to this work. This project has at times been an arduous journey, and there have been a number of people that contributed to it.

Dr. James Johnson and Dr. Graham King have been of prodigious assistance throughout this project. Their investment in me and in this project has been tremendous. Through working with them and their team, I learned the correct way of doing research, writing a grant application, and writing manuscripts.

Other people have been of significant assistance. Dr. Ferreira has been a key member in every step of this decade long journey, Dr. Athwal for his time in the lab as well as assistance with the manuscripts, Josh Giles, Simon Deluce, Allison Pellar, Emily Lalone, and Hannah Shannon all so helpful in the lab as well as sources of positive energy. A special thanks to Emily Engbers for her artistic contributions to this manuscript and to Clayton Cook and the University Machine Services team for their expertise and assistance building the simulator.

The project was funded by a generous grant from Physicians' Services Incorporated Foundation. Thank you to this organization for making this possible.

I'd also like to thank my wonderful wife and children for their patience and encouragement during this journey. My parents and siblings for their encouragement and advice. My wife's family has also been supportive. Finally, I'd like to thank God for the opportunity and for what I needed for this project.

Table of Contents

List of Tables

List of Figures

List of Appendices

Chapter 1

Overview: *The goal of this chapter is to explain the anatomy, biomechanics and function of the soft tissue and bone anatomy of the forearm. Forearm injuries and the current treatments for these injuries are reviewed, with a focus on radial head fractures. A review of the testing protocols and their potential limitations are also discussed. The objectives, hypothesis and rationale of the project are summarized.*

1.1 Anatomy of the Forearm

1.1.1 Osseous Anatomy of the Forearm

1.1.1.1 Forearm Osteology

The forearm is a complex relationship of two bones: the radius and the ulna (Fig 1.1). This relationship is intricate, and any deviation in either bone alters the articulations present at either end. The radius possesses a radial bow that is at its maximum at 60% of the length of the radius and is 10% of the length of the radius at maximal magnitude [1]. This has measured at mean maximal value of 15.3 mm of radial bow in the normal arm [2]. Deviation of greater than 2.8mm from the mean radial bow has been shown to cause rotation of the forearm to be less than 80% of the normal side [2]. Normal pro/supination motion is approximately 77° of pronation, and 72° of supination [3] (Fig 1.2).

Motion between the radius and ulna occurs in the rotational plane through pro/supination, as controlled by the fibrous interosseous membrane (IOM) and terminal articulations between each bone (Fig 1.1). The radius and ulna articulate at the proximal end at the elbow to allow flexion/extension, and at the wrist to allow circumduction.
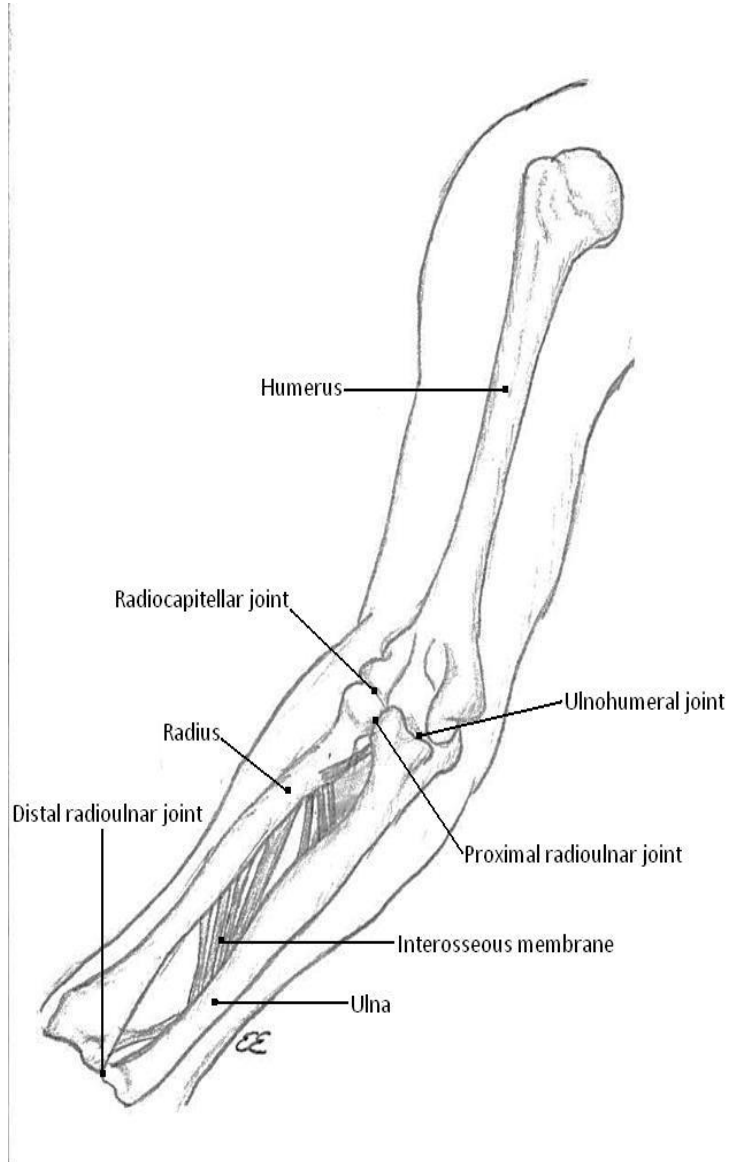
Figure 1.1: Upper Extremity Structure
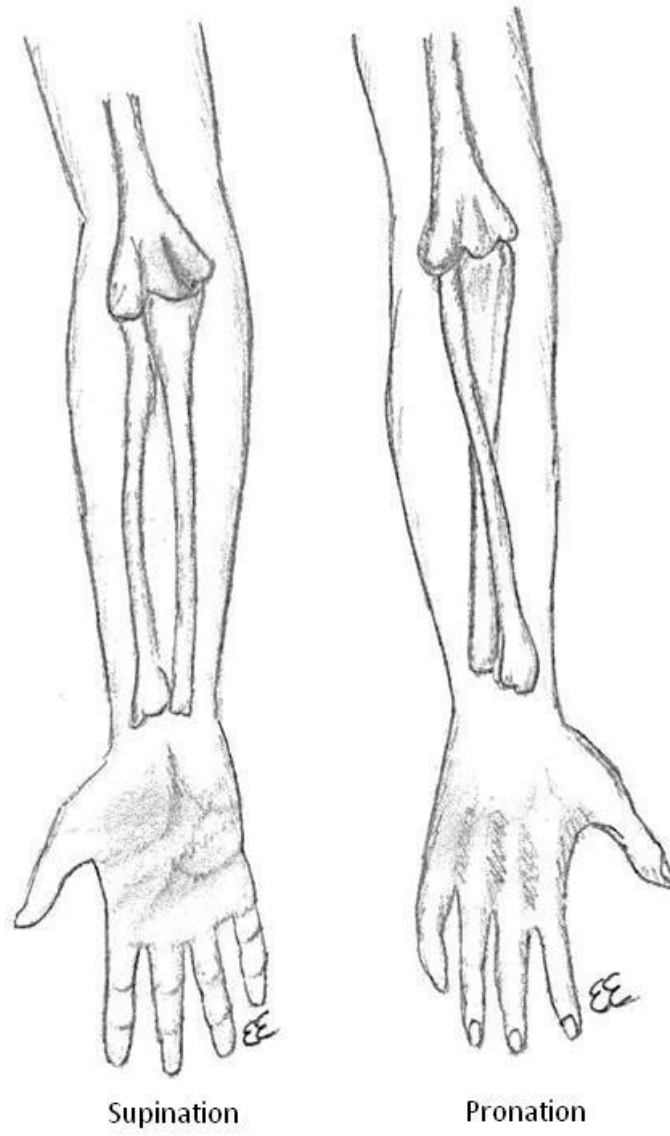
Figure 1.2: Forearm Rotation

1.1.1.2 Wrist Osteology

     The wrist joint is comprised of a complex interaction of the five metacarpals, eight carpals and two forearm bones (Fig 1.3). The interaction of these bones participates in the intricate function of the wrist; assisting in positioning the hand in space [4] [5]. The wrist allows motion in flexion/extension, ulnar and radial deviation, and finally contributes to pronation/supination; in order of decreasing magnitude [6] [7] [8] (Fig 1.4). The normal motion of the wrist is 65-80° of flexion, 65-80° of extension, 10-20° of radial deviation, 20-35° of ulnar deviation and 5-15° of pro/supination [4].
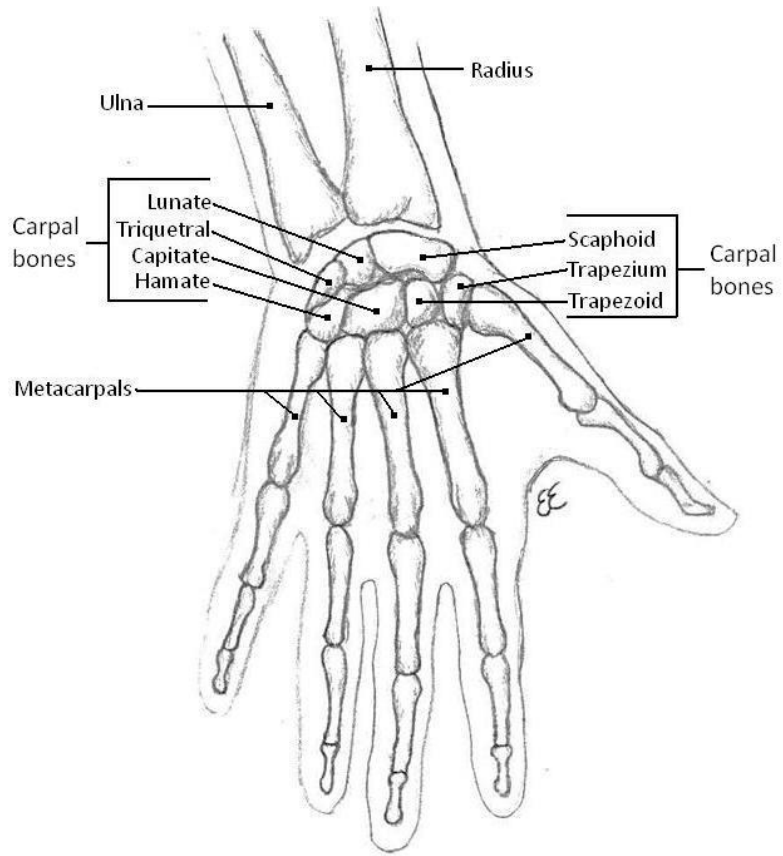
Figure 1.3: Wrist Osteology
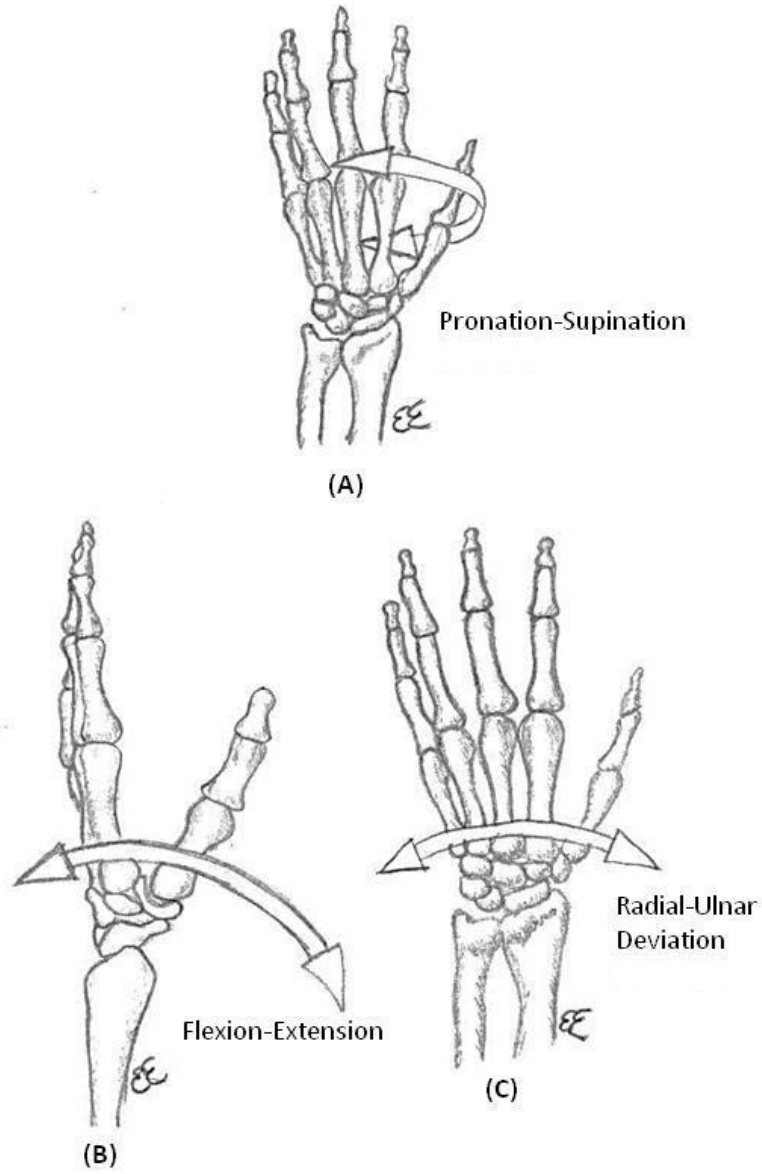
Figure 1.4: Wrist Range of Motion

1.1.1.3 Distal Radio-Ulnar Joint Osteology

The Distal RadioUlnar Joint (DRUJ) is the distal articulation of the forearm unit. It permits both pivoting and translational motions to allow forearm pronation and supination (Fig 1.5) [9]. The ulnar head has articular cartilage encompassing 90-135° of its circumference to allow articulation within the sigmoid notch of the distal radius [10]. The distal surface of the ulna is convex and is also covered with articular cartilage [10].

At the DRUJ, the radius of curvature of the sigmoid notch is 4-7 mm greater than the 10 mm of ulnar head curvature, and has a curvature of 47-80° [10]. The ulnar head has an average inclination of 20° to the shaft of the ulna; as does the sigmoid notch [10]. As can be inferred from the lack of congruity, stability is provided by the soft tissues surrounding the joint including the TFCC (triangular fibrocartilage complex). The distal radius is comprised of the scaphoid and lunate facets as well as the sigmoid notch (Fig 1.6).
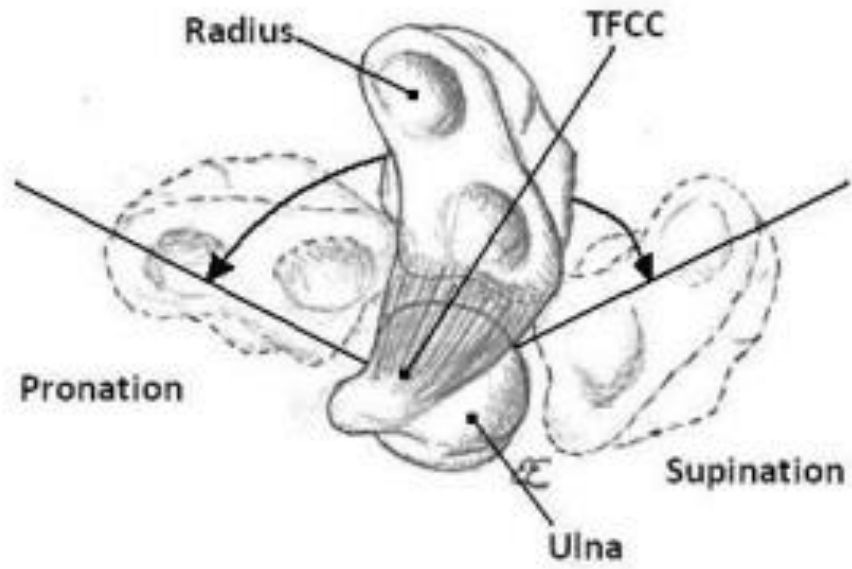
Figure 1.5: Distal Radio-Ulnar Joint Pro/Supination, Axial View
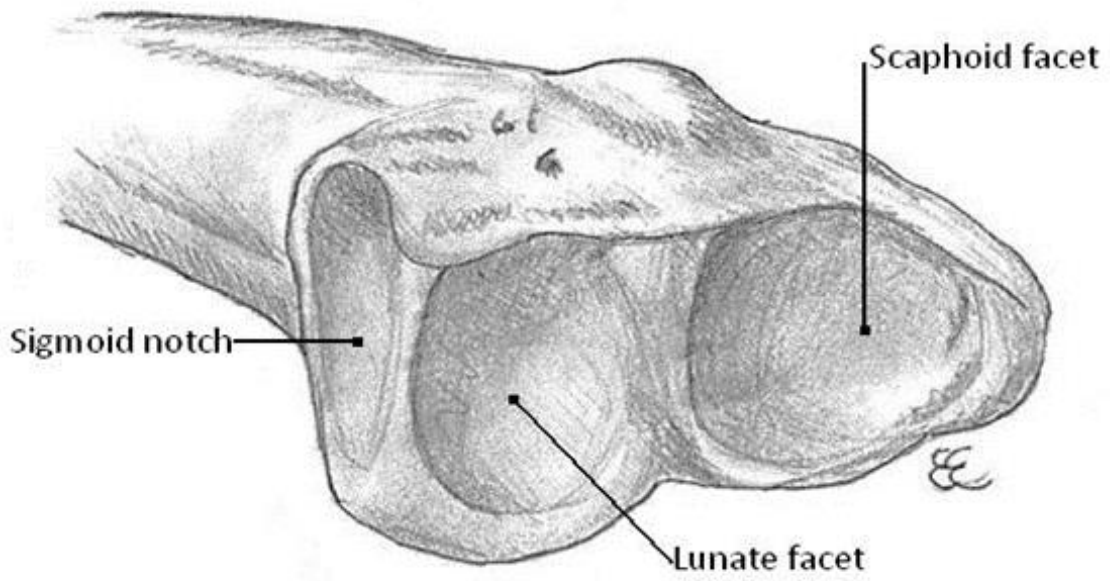
Figure 1.6: Distal Radius Articulation

1.1.1.4 Elbow Osteology

The elbow is made up of the articulation of three bones; the ulna, radius and humerus. The articulations are the ulnohumeral, radiocapitellar and the proximal radioulnar joints (Fig 1.1). The radial head is elliptical in shape [11] [12]. The proximal articular surface is concave and appropriately referred to as the radial dish. Articular cartilage covers 240° of the outer margin (Fig 1.7). The proximal ulna is complex and is comprised of the radially directed lesser sigmoid notch and the humeral directed greater sigmoid notch. The greater sigmoid notch terminates at the olecranon tip proximally and the coranoid tip distally. The distal humerus flares out to form the epicondyles medially and laterally with the central depression called the coronoid fossa anteriorly and the olecranon fossa posteriorly. The articular components are the spherical capitellum radially and the spool shaped trochlea ulnarly (Fig. 1.8).

The radiocapitellar joint is comprised of the articulation between the radial head, with the capitellum. This joint is designed to allow axial loading while pivoting with pronation and supination as well as gliding for flexion and extension.

The ulnohumeral joint consists of the articulation of the trochlea within the greater sigmoid notch. The coronoid and olecranon tips correspond to their respective fossae of the humerus at the extremes of flexion and extension.

The Proximal Radioulnar Joint (PRUJ) is formed by the outer articulation of the radial head within the lesser sigmoid notch; a pivoting joint to allow pronation and supination (Fig 1.7).
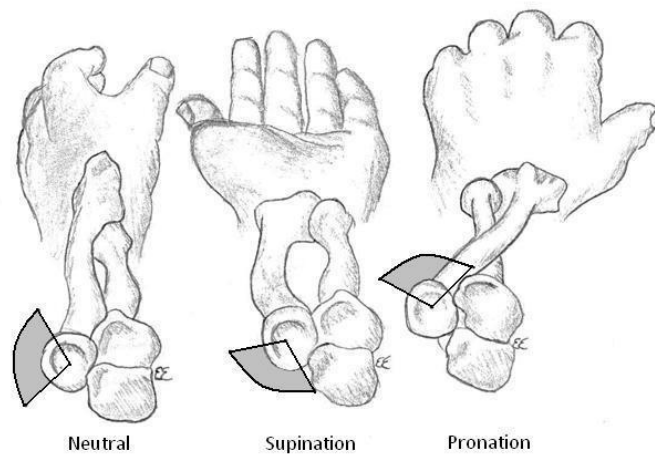
Figure 1.7: PRUJ Articulation
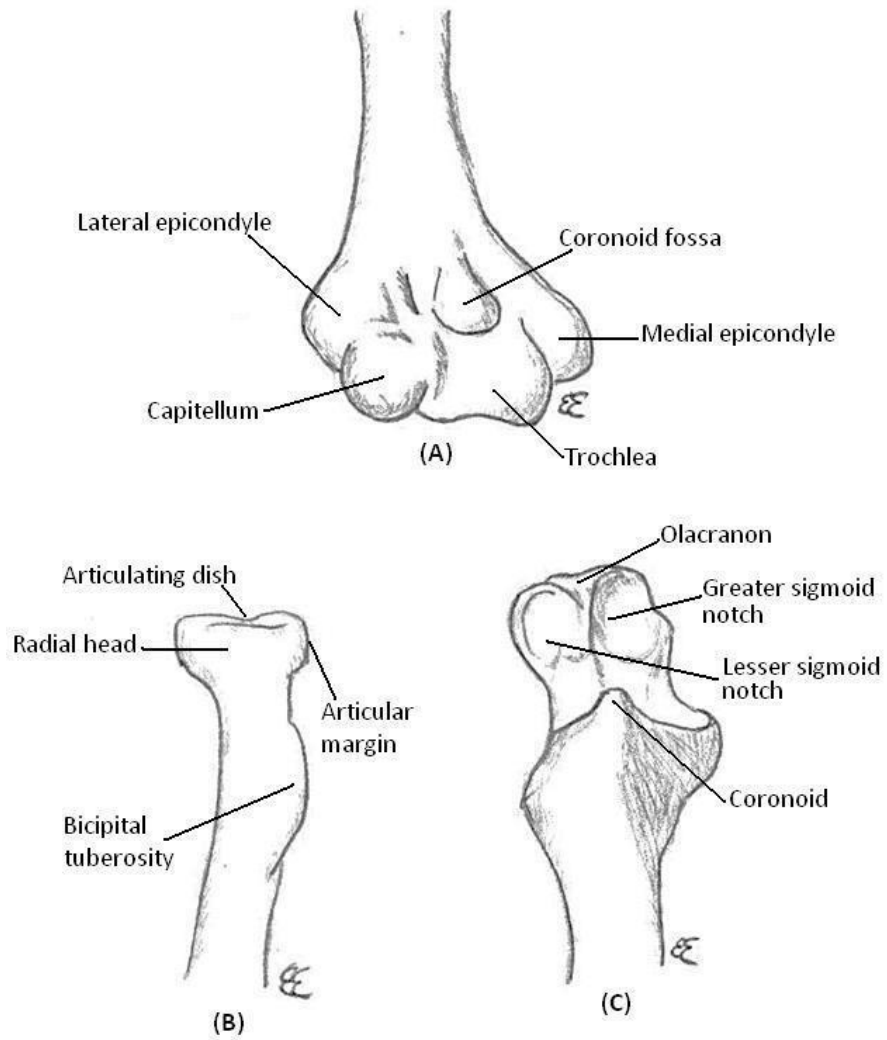
Figure 1.8: Elbow Osteology

1.1.2 Soft Tissue Anatomy of the Forearm

1.1.2.1 Wrist Ligaments

The distal surface of the ulna is convex and is covered by the triangular articular disc [4]. The triangular articular disc in conjunction with associated ligaments makes up the triangular fibrocartilage complex (TFCC) [13]. The superficial dorsal and volar radioulnar ligaments insert into ulnar styloid [4] (Fig 1.9). The deep portions of the radio-ulnar ligaments insert in the roughened area at the base of the styloid called the ulnar fovea [13]. The radioulnar ligaments originate at the dorsal and volar lip of the radial sigmoid notch. The dorsal radioulnar ligament inserts into the ECU subsheath, and tends to be thicker than the palmar radioulnar ligament [14]. The TFCC also attaches to the ulnotriquetral and ulnolunate ligaments [13].

The literature indicates that 20% of the distal radioulnar joint stability is provided by osseous congruity, with the remainder provided by soft tissue [15]. Maximal stability is in neutral, and increased pronation and supination diminishes stability[11]. The roles and contribution to each soft tissue element is controversial. Some literature indicates that in full pronation, the volar radioulnar ligaments are taut and the dorsal lip of the sigmoid notch is in contact with the ulnar head. In full supination, the dorsal radioulnar ligaments are taut and the volar lip of the sigmoid notch is in contact [17] [15] [10]. Others have found that the dorsal ligament is taut and is important in pronation while the volar ligament has an equally important role in supination [18] [19]. Overall it is recognized that the radio-ulnar ligaments have an important role in maintaining DRUJ stability [10]. Some have shown that the TFCC is important to stabilize the DRUJ in neutral rotation, while the IOM is important in pronation and supination [20]. Other important soft tissue

stabilizers include the ECU sheath [21], however, other authors have found that the ECU sheath has little impact on stability [15].

1.1.2.2 Interosseous Membrane

The interosseous membrane (IOM) is a complex structure. It has also been called the interosseous ligament, indicating it's similar characteristics to a ligament [22] and the interosseous ligament complex [23]. It has five discrete components; the central band (CB), accessory band (AB), distal oblique bundle (DOB), proximal oblique cord (POC) and the dorsal oblique cord (DOC) [24] [25] (Fig 1.10). These bands are not consistently present, with the central band, accessory band and proximal oblique cord being seen in all specimens but the dorsal oblique accessory cord and distal oblique bundle only being seen in approximately 50% of cadavers in one study [25]. The central band is 9.7 mm (4.4-16) wide, and 1.3 mm (1-1.6) thick. In terms of orientation, the CB has been found to be at a 21 to 24° angle relative to the shaft of the ulna [22]. It has a greater length of insertion on the ulna (42 – 46 mm) than the radius (34-42 mm) [22].

In contrast with the substantial thickness of the CB, the AB is less than one mm in thickness, but varies in number from one to 5 ligaments. The DOB is 4.4 mm (2-6) wide and 1.5 mm (0.5-2.6) thick on average. The POC is 3.7 mm (1.5-8) wide and 1.1 mm (0.4-2) thick, similar to that of the dorsal oblique accessory cord of 3.2 mm (1.9-5) wide and 0.9 mm (0.5-1) thick [25].

Biochemically, the IOM is made up of collagen with a supporting framework of elastin, to withstand large loads [24].
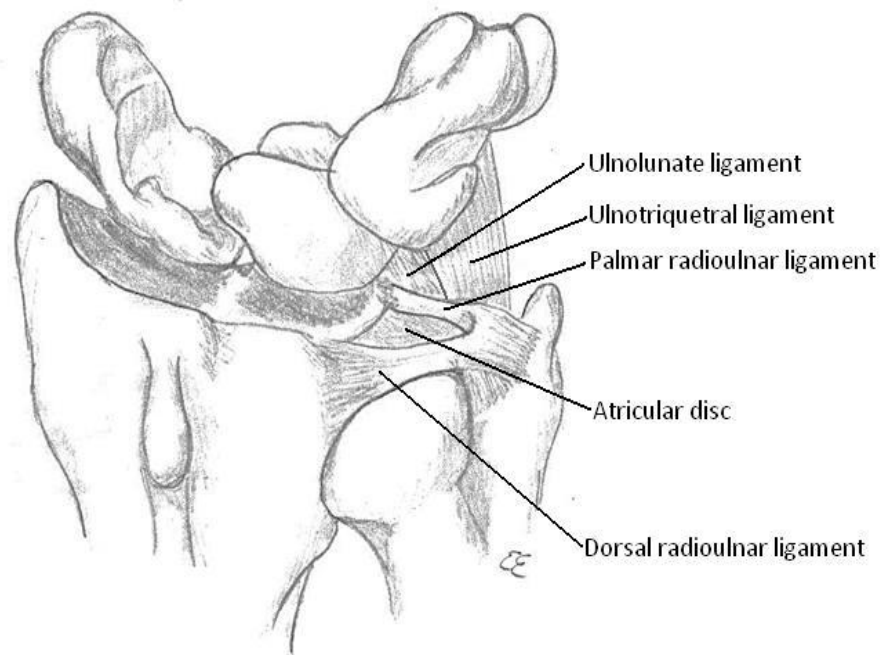
Figure 1.9: The Wrist, TFCC and Ligaments
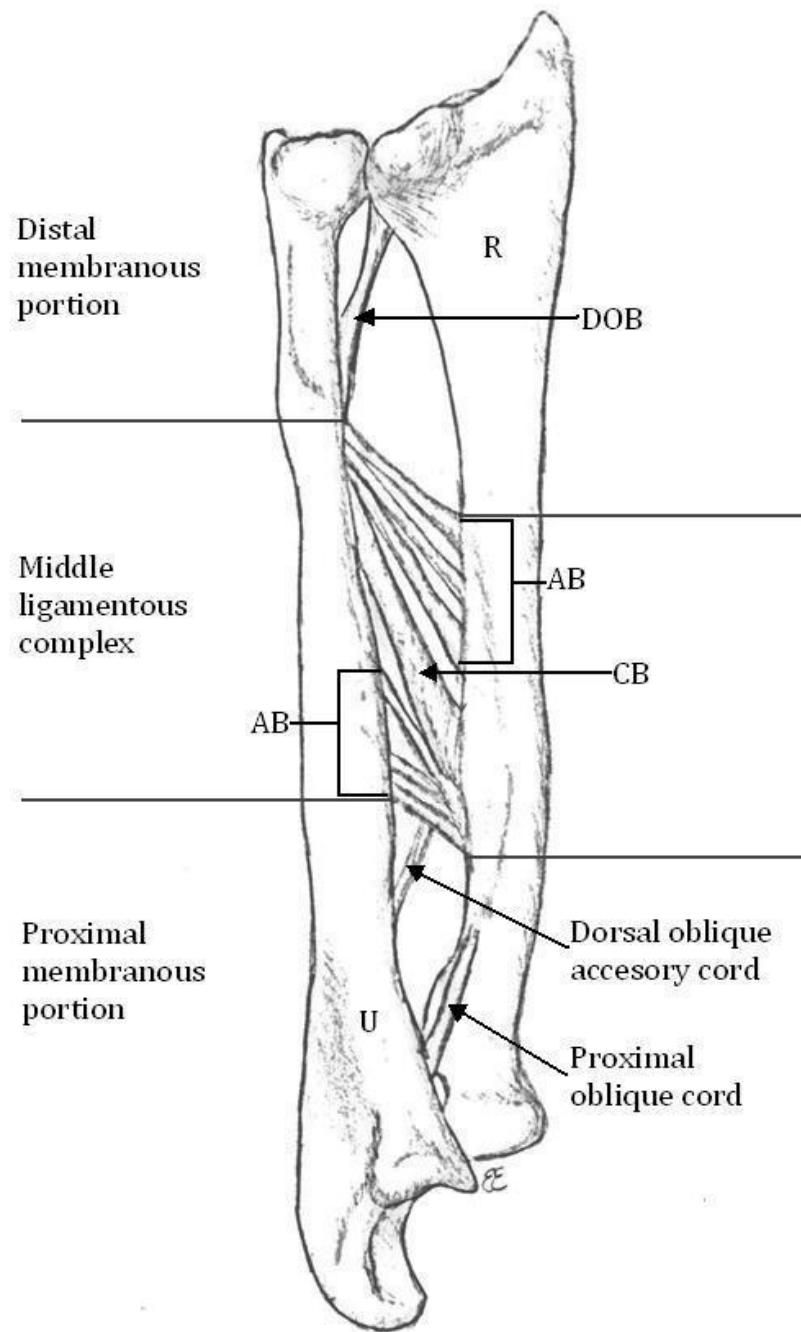
Figure 1.10: Anatomy of the IOM

1.1.2.3 Elbow Ligaments

The soft tissue stabilizers of the elbow include the joint capsule and collateral ligaments. The joint capsule has medial and lateral thickenings that form the medial and lateral collateral ligaments [26] (Fig 1.11). The medial collateral ligament is comprised of the anterior, middle and transverse segments which emanate from medial epicondyle [27]. The medial collateral ligament is an important valgus stabilizer. The anterior bundle is especially important, and is composed of the anterior and posterior bands [28].   The lateral collateral ligament is harder to differentiate from the capsule. It is made up of the annular ligament, the radial and lateral ulnar collateral ligaments. The radial collateral ligament originates at the lateral epicondyle and inserts into the annular ligament. The lateral ulnar collateral ligament (LUCL) is an important stabilizer for varus and posterolateral rotatory loading. Originating at the lateral epicondyle, it inserts on the crista supinatoris [29].
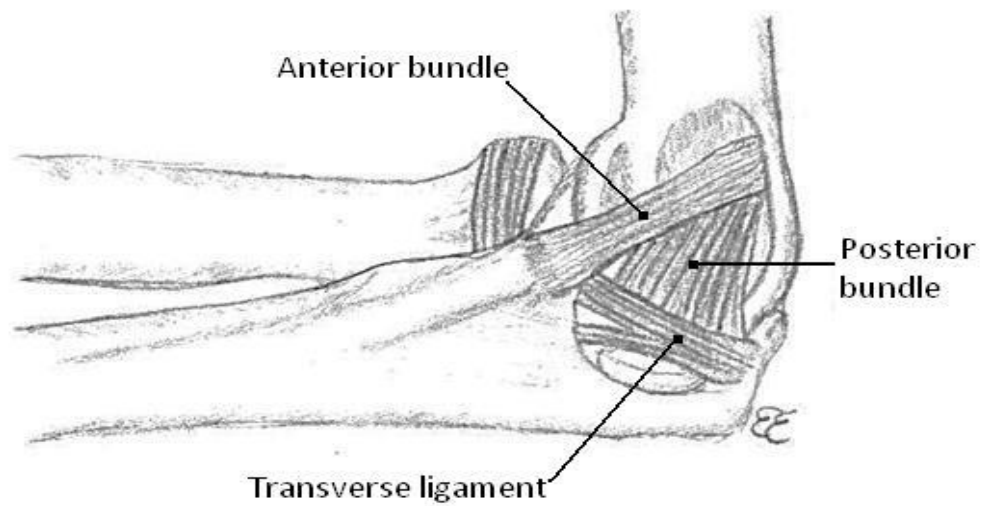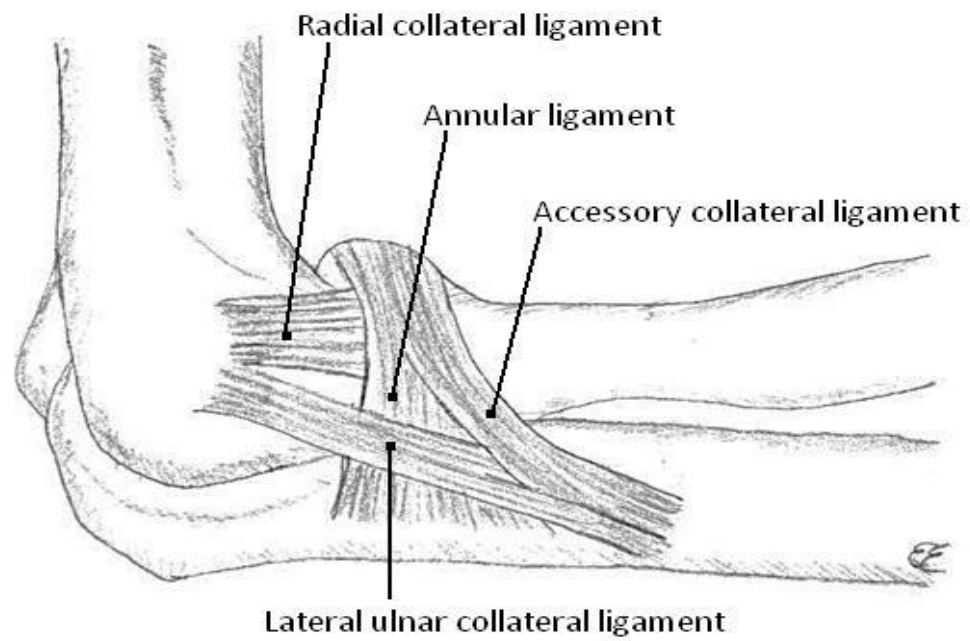
Figure 1.11: Important Elbow Ligaments

1.1.2.4 Muscles

A large number of muscles are involved in the functioning of the forearm as a unit and specifically the elbow and wrist joints. Crossing the elbow are 24 musculotendinous units (Table 1), of which the primary muscles of interest in elbow flexion and extension are the biceps and triceps respectively. There are 29 musculotendinous units cross the wrist [30] (Table 2). Of these, the musculotendinous units of primary interest for wrist motion are the flexor carpi radialis, flexor carpi ulnaris, extensor carpi ulnaris and the extensor carpi radialis longus and brevis [31]. (Fig 12) The forearm itself is stabilized by active units; in particular both the pronator quadratus and teres as well as the supinator stabilize the forearm and may alter the loads on the IOM.

Table 1: Musculotendinous Units crossing the Elbow

Action	Muscles
Flexion	Brachialis Biceps brachii Brachioradialis Pronator teres Flexor carpi ulnaris
Extension	Triceps Anconeus
Supination	Supinator Brachioradialis Biceps brachii
Pronation	Pronator quadratus Pronator teres Flexor carpi radialis
Wrist flexion	Flexor carpi radialis

	Flexor carpi ulnaris
Wrist extension	Extensor carpi radialis longus
	Extensor carpi radialis brevis
	Extensor carpi ulnaris

Table 2: Musculotendinous Units that cross the Wrist

Action	Muscles
Supination	Supinator, Biceps Brachii
Extension	Extensor carpi radialis longus, Extensor carpi radialis brevis, Extensor carpi ulnaris
Flexion	Flexor carpi radialis longus, Flexor carpi radialis brevis, Flexor carpi ulnaris
Ulnar Deviation of Wrist	Flexor carpi ulnaris, Extensor carpi ulnaris
Radial Deviation of Wrist	Flexor carpi radialis, Extensor carpis radialis longus, Abductor pollicis longus, Extensor pollicis brevis
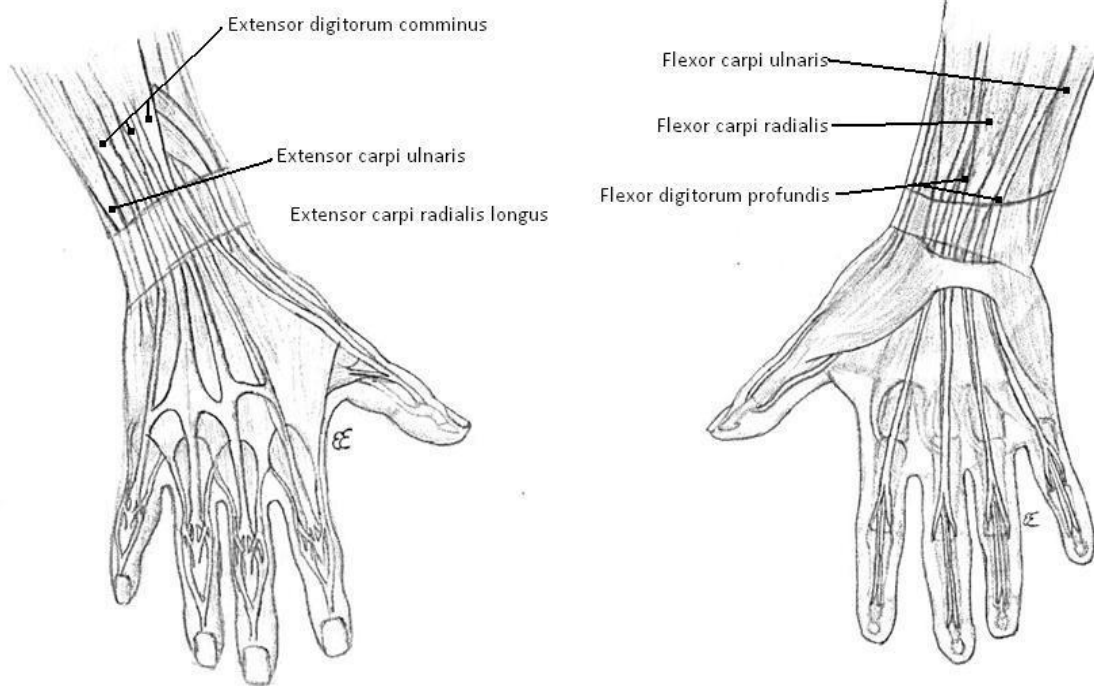
Figure 1.12: Important Musculotendinous Units that Cross the Wrist

1.2 Biomechanics of the Forearm

1.2.1 Axes of Motion

1.2.1.1 Axis of Elbow Flexion and Extension

The kinematic axis of flexion/extension of the ulna with respect to the humerus has been found to be 84º [32], 82-86º [33], 80º [34] or 86º [35] in the frontal plane. However, other authors found that the axis of flexion/extension does not have a fixed position [36]. The position of this axis was found to be located within the instant center of rotation in circles of 3 and 1 mm in diameter on the lateral and medial sides of the elbow, respectively [34]. The screw displacement axis (SDA) has been descriptively located from the anterior aspect of the medial epicondyle, the center of the trochlea, and the center of the projection of the capitellum onto a parasagittal plane [35]. The position of the flexion axis moved with individual variations ranging from $2.1°$ (-1° to 1°) to $14.3°$ (-6.5° to 8°) in the frontal plane and from $1.5°$ (-1° to 0°) to $10°$ (-3° to 7°) in the horizontal plane [36]. Others found variations of lesser magnitude of $2.5° \pm 1.0°$ in the frontal and $6° \pm 2°$ in the horizontal plane [35]. However, the ultimate position of the flexion axis has been found to have a distal medial inclination in most studies, with a relatively small locus of instant center of rotation [32] [35] [37]. This has resulted in the alignment being in valgus in extension and varus in flexion.

1.2.1.2 Axis of forearm rotation

The axis of rotation of the forearm runs from the fovea of the ulnar head, proximally

through the center of the radial head [3]. For the distal ½ of the ulna, the axis of rotation

falls on the ulnar insertion of the IOM. More proximally, it runs through the center of the

IOM but runs through the shaft of the radius proximally. This conceptually supports the

CB, distal AB and DOB as being isometric and the POC and DOC lacking isometry [3].

As the forearm pronates, the radius moves proximally, and in supination it moves

distally. This proximal/distal motion has a magnitude of about 1.3 mm [38]. The DRUJ

also allows dorsal/palmar motion, as seen by dorsal movement of the radius with

pronation, and volar movement with supination [7] [16] [39]. This translation is

increased if the soft tissues are disrupted [16]. Although sectioning of the annular

ligament increases the mediolateral motion of the radius with respect to the capitellum, it

does not effect the axis of rotation of the forearm [40].

1.2.2 Biomechanics of the IOM

The IOM has two main roles; load transmission and stabilization of the radio-ulnar

articulations [41]. The IOM has an oblique orientation of the fibers with respect to the

radius and ulna, with the CB at a 21 to 24º angle relative to the shaft of the ulna [22].

The IOM's primary function is to transmit load in the direction of the IOM. This can be

particularly seen in that the load to failure in the longitudinal axis has been found to be

120N while only 0.82N in the transverse direction [42]. The magnitude of the load

transferred by the IOM has been reported to be greater than 1000 N [43]. A significant

portion of this load is transmitted by the CB as the CB is three times stronger than the

remaining components of the IOM [44].

While one study reported that the IOM was isometric [3], most authors have measured

changes in IOM strain during forearm rotation. This majority in literature is consistent

with the anatomy of the forearm as the IOM is a ligament. Ligaments can be expected to

tolerate more strain than other physiologic structures such as tendons. Some studies have

reported the IOM to be at highest strain in supination [45] [46], while others found the

highest strain in neutral [47]. The lowest strain has been reported in pronation [46] [47]

or in neutral rotation [48]. However, the translation of the ulna with respect to the radius

also needs to be considered as having a role in the loads transmitted by the IOM and the

position of the maximum tension.

In addition to its role as an axial stabilizer, the IOM also prevents divergence of the

radius and ulna [41]. If the IOM is partially or completely sectioned, there is resultant

DRUJ instability [49]. In particular, the distal IOM is found to have a key stabilizing role

[50], with the DOB of particular importance (although it is only present in 40% of the

population) [3].

1.2.3 Forearm Load Transmission

The biomechanics of load transmission within the forearm are extremely complex. As

the IOM both transmits load as well as maintains the radio-ulnar articular relationships,

IOM strain is affected by forearm loads applied as well as the position of the forearm.

However, grossly it has been seen that the radiocarpal joint transmits approximately 80%

of the applied load and the ulnocarpal joint approximately 20% of the loads applied at the

wrist [51] [52]. Other authors list greater forces transmitted by the ulnocarpal joint at the wrist of up to 30-40% of the applied load [8] [53]. However, proximal loads have been found to be 50% at the radius and 50% at the ulna, indicating load transfer via the IOM [53]. The forearm loading characteristics may be affected by the rotational position, with greater contact area at the radiocapitellar joint in supination than in pronation [16].

1.2.4 Forearm Loading

Current in-vitro studies of forearm load transfer use forces of 100-136 N in general with the upper limits meant to represent loading of 30 lbs through the elbow joint [45] [48] [54]. The literature, however, suggests that higher loads occur in vivo. In vivo analysis has indicated maximal loads at the ulnohumeral articulation of 1600 N, radiohumeral of 800 N and wrist joint loads of 2800 N at moderate activity [55]. Other literature demonstrates ulnohumeral loads of 3200 N with heavy lifting [56] or 2450 N and radiohumeral loads of 1500 N [57] under single repetition maximal contraction loading. Proportionality was found in other studies, indicating that the ulnohumeral loads were 0.3-0.5 X body weight for ADL's [58].

1.3 Forearm Injuries

1.3.1 Essex-Lopresti Injuries

The Essex – Lopresti injury was relatively recently described. Brockman in 1930 first described proximal translation of the radius with respect to the ulna after a radial head fracture [59]. Curr and Coe subsequently described an acute dislocation of the distal radioulnar joint (DRUJ) after a radial head fracture [60]. Essex-Lopresti described two

cases of a fractured radial head and acute DRUJ instability and associated it with an IOM lesion [61].

An Essex-Lopresti injury is classically described as a radial head fracture, with IOM disruption and DRUJ instability wheras a Monteggia injury is a fracture of the ulna with dislocation of the radiocapitellar joint. The nomenclature is clouded, with some stating that radioulnar dissociation is the acute form of this injury and an Essex-Lopresti injury is the more chronic form [44]. In addition to the obvious pathology at the radial head, physical exam of these patients may reveal tenderness diffusely over the forearm and the ulnar side of the wrist as well as forearm ecchymosis [44]. A bony variant has been described, with a fracture associated with the DRUJ injury. This ulnar head fracture resulted in instability similar to the soft tissue instability seen classically, and was repaired with internal fixation [62].

The classic definition of an acute Essex-Lopresti requires surgical management as a chronic Essex-Lopresti injury that was initially missed can result in significant patient disability and are often difficult to treat [63]. However, the surgical algorithm is unclear. Options include radial head restoration, either with internal fixation or with arthroplasty for longitudinal instability, and DRUJ instability can be treated by pinning the joint or by reconstruction of capsular tissue and the TFCC [64]. Reconstructions of the IOM in vivo have been described, but are technically challenging and there are few reported cases [65]. The controversy of treatment is partially due to the fact the load transfer within the forearm is unclear, and a greater understanding of the biomechanics of the forearm is required.

1.3.2 Radial Head Fracture

Radial head fractures are a frequent injury and are the most common fractures of the elbow [66]. These fractures can have significant repercussions for the patient, with chronic pain, stiffness, osteoarthritis, wrist symptoms, weakness and valgus alignment are potential residua of the injury [67]. The classification of a radial head fracture remains problematic, but most rely on some variant of the original description by Mason (Fig 1.13). This system uses a three tiered system, with a type-I being undisplaced, a type II having displaced wedge fragment(s), and type III being comminuted [27].
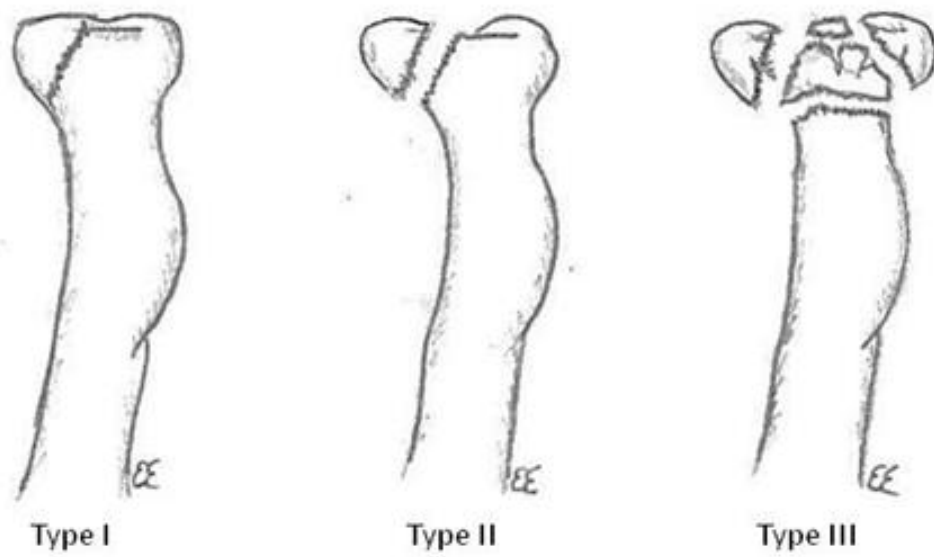
Figure 1.13: Mason Classification

As outcomes are often suboptimal for open reduction internal fixation of type III fractures [69], these fractures are commonly treated with radial head excision or arthroplasty. Soft tissue disruptions which have been reported in up to 75% of patients with comminuted radial head fractures [70] hence radial head arthroplasty is recommended to increase elbow stability [71]. Radial head excision has been reported to have a high incidence of late instability and arthritis [72]. Interestingly, the IOM is abnormal on MRI in 2/3rds of Mason I fractures, suggesting the IOM can be injured even with minimal trauma to the radial head [73]. In a case series of 20 patients presenting with Essex-Lopresti injuries, 15 had a radial head excision without knowledge of the IOM injury. While the clinical impact of IOM injuries has not been completely understood; missed Essex-Lopresti injuries often lead to suboptimal outcomes.

1.3.3 Radial Head Fracture Treatment: Arthroplasty

Research on radial head arthroplasty (RHA) has been focused on the effect of discrepancies in length of the prosthesis on forearm biomechanics, with little work on the effect of diameter (Fig. 1.14) RHA with inadequate length results in increased distal ulnar loads and increased proximal radial displacement, with the resultant recommendation by some to err on over lengthening [74]. Other investigators have reported that in an MCL deficient elbow, increased length reduced laxity, but increased contact forces, while decreased length increased laxity and ulnar rotation [75] [76]. Although studies indicate the importance of radial head length, it does not quantify the load changes of the forearm. Also, the effect of diameter of the RHA has not been reported. How this dimension impacts the contact area or forces at the radiocapitellar articulation and on IOM biomechanics and forearm load transfer is also unknown. The

(A)

(B)
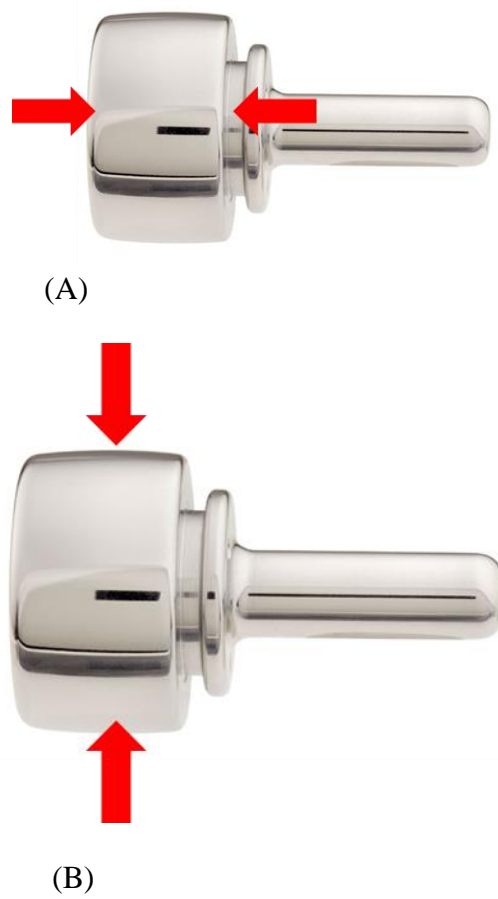
Figure 1.14: Radial head dimensions of length (A) and diameter (B)

effect of a change in radial head length or diameter on the forearm's resistance to rotation is unknown.

1.4 Current Biomechanical Studies of the Forearm

In-vitro testing of forearm biomechanics has been limited in a number of ways, making the clinical generalizability of their results limited. Most studies have been performed under static loading, often at a single fixed position of elbow flexion. Other limitations include invasive load cells that require sectioning of the radius or ulna, significant soft tissue stripping, or non-reproducible loading systems. Measurement techniques require optimization, and loads are often applied in a non-physiologic manner. Also, testing has been almost exclusively limited to axial loading scenarios; the effect on rotation of the forearm through pronation and supination has not been studied. How the radial head state (native, excised or RHA properties) impacts the ability of the forearm to rotate is unknown. Improvements in in-vitro testing techniques are required in an effort to develop clearer indications for surgery and to make advances in prosthetic devices.

1.5 Thesis Rationale

The forearm is a complex articular unit, comprised of the movement of the radius and ulna both in relation to themselves as well as with the carpal bones and the humerus. Proximally there is articulation at the elbow and the PRUJ, and distally at the wrist and the DRUJ. The complex relationship of the radius and the ulna is linked by the IOM, and the forearm could be considered as a single articular unit. However its biomechanics are poorly understood in a static situation; much less a kinematic situation.

Testing of a specific area of interest on a cadaveric specimen is a balance of physiologic motion and appropriate constraint. Maintenance of the cadaveric specimen's integrity as well as testing at physiologically meaningful loads are challenges. Also, quantification of IOM loads is difficult, and often inferred in an indirect manner. The development of a simulator and physiologic testing algorithm will allow forearm testing in a clinically meaningful manner.

In addition to a lack of a basic understanding how the native forearm functions, the effect of changes to the radial head on forearm biomechanics are not well delineated. To date studies on axial load transfer within the forearm have been limited by non-physiologic testing parameters. To provide a greater understanding on some of the clinical outcomes seen for RHA, a better understanding is needed on how changes to the dimensions of the radial head – length and diameter – impact load transfer and radiocapitellar articular properties. Comparison of the native radial head, radial head excision and radial head arthroplasty dimensions on forearm biomechanics is important to provide a better understanding on the clinical impact of specific treatment algorithms.

1.6 Objectives

The objectives for this study were:

1. To create an upper extremity simulator that would provide a means of forearm testing in a repeatable and reproducible way both in dynamic and static loading conditions.

2. To examine the effect of radial head state (native vs excision vs arthroplasty) on IOM tension

3. To examine the effect of radial head implant length on IOM tension, radiocapitellar force and radiocapitellar contact area.

4. To examine the effect of radial head implant diameter on IOM tension, radiocapitellar contact force and radiocapitellar contact area.

1.7 Reference List

[1]   Lincoln TL, Mubarak SJ: "Isolated" traumatic radial-head dislocation. J Pediatr Orthop 14:454-457, 1994.

[2]   Firl M, Wunsch L: Measurement of bowing of the radius. J Bone Joint Surg Br 86:1047-1049, 2004.

[3]   Schemitsch EH, Richards RR: The effect of malunion on functional outcome after plate fixation of fractures of both bones of the forearm in adults. J Bone Joint Surg Am 74:1068-1078, 1992.

[4]   Moritomo H, Noda K, Goto A, Murase T, Yoshikawa H, Sugamoto K: Interosseous membrane of the forearm: length change of ligaments during forearm rotation. J Hand Surg Am 34:685-691, 2009.

[5]   Berger RA: The anatomy and basic biomechanics of the wrist joint. J Hand Ther 9:84-93, 1996.

[6]   Bray TJ, Simpson LA: Techniques in Fracture Fixation. Gower Medical Publishing, 1993.

[7]   Green DP: Carpal dislocations and instabilities. pp. 861-928. In Green D (ed): Operative Hand Surgery. Churchill Livingstone; New York, 1993.

[8]   King GJ, McMurtry RY, Rubenstein JD, Gertzbein SD: Kinematics of the distal radioulnar joint. J Hand Surg Am 11:798-804, 1986.

[9]   Palmer AK, Werner FW, Murphy D, Glisson R: Functional wrist motion: a biomechanical study. J Hand Surg Am 10:39-46, 1985.

[10]   Hagert CG: The distal radioulnar joint in relation to the whole forearm. Clin Orthop Relat Res56-64, 1992.

[11]   Linscheid RL: Biomechanics of the distal radioulnar joint. Clin Orthop Relat Res 46-55, 1992.

[12]   thiemeteachingassistant.com. DRUJ Imaging. 2010.

Ref Type: Internet Communication

[13]   af Ekenstam F: Anatomy of the distal radioulnar joint. Clin Orthop Relat Res14-18, 1992

[14]   Scheer JH, Adolfsson LE: Pathomechanisms of ulnar ligament lesions of the wrist in a cadaveric distal radius fracture model. Acta Orthopaedica 82(3), 2011

[15]   Berger RA: The anatomy of the ligaments of the wrist and distal radioulnar joints. Clin Orthop Relat Res32-40, 2001

[16]   Pfirrmann CW, Theumann NH, Chung CB, Botte MJ, Trudell DJ, Resnick D: What happens to the triangular fibrocartilage complex during pronation and supination of the forearm? Analysis of its morphology and diagnostic assessment with MR arthrography. Skeletal Radiol 30:677-685, 2001

[17]   af Ekenstam F: Anatomy of the distal radioulnar joint. Clin Orthop Relat Res14-18, 1992

[18]   af Ekenstam F: Anatomy of the distal radioulnar joint. Clin Orthop Relat Res14-18, 1992

[19]   Shaaban H, Giakas G, Bolton M, Williams R, Wicks P, Scheker LR, Lees VC: Contact area inside the distal radioulnar joint: effect of axial loading and position of the forearm. Clin Biomech (Bristol , Avon) 22:313-318, 2007

[20]   King GJ, Zarzour ZD, Patterson SD, Johnson JA: An anthropometric study of the radial head: implications in the design of a prosthesis. J Arthroplasty 16:112-116, 2001

[21]   van Riet RP, Van Glabbeek F, Neale PG, Bortier H, An KN, O'Driscoll SW: The noncircular shape of the radial head. J Hand Surg Am 28:972-978, 2003

[22]   Wrist: TFCC and ligamentous structures. 2010.

Ref Type: Internet Communication

[23]   Ishii S, Palmer AK, Werner FW, Short WH, Fortino MD: An anatomic study of the ligamentous structure of the triangular fibrocartilage complex. J Hand Surg Am 23:977-985, 1998

[24]   Berger RA: The ligaments of the wrist. A current overview of anatomy with considerations of their potential functions. Hand Clin 13:63-82, 1997

[25]   af Ekenstam F: Anatomy of the distal radioulnar joint. Clin Orthop Relat Res14-18, 1992

[26]   Stuart PR, Berger RA, Linscheid RL, An KN: The dorsopalmar stability of the distal radioulnar joint. J Hand Surg Am 25:689-699, 2000

[27]   Mason ML. Some observations on fractures of the head of the radius with a review of one hundred cases. Br J Surg 1954;42:123-32.

[28]   af Ekenstam F, Hagert CG: The distal radio ulnar joint. The influence of geometry and ligament on simulated Colles' fracture. An experimental study. Scand J Plast Reconstr Surg 19:27-31, 1985

[29]   Olerud C, Kongsholm J, Thuomas KA: The congruence of the distal radioulnar joint. A magnetic resonance imaging study. Acta Orthop Scand 59:183-185, 1988

[30]   Schuind F, An KN, Berglund L, Rey R, Cooney WP, III, Linscheid RL, Chao EY: The distal radioulnar ligaments: a biomechanical study. J Hand Surg Am 16:1106-1114, 1991

[31]   Kapandji IA: The Physiology of the joints. Churchill Livingstone, Edinburgh, 1982

[32]   King GJ, McMurtry RY, Rubenstein JD, Ogston NG: Computerized tomography of the distal radioulnar joint: correlation with ligamentous pathology in a cadaveric model. J Hand Surg Am 11:711-717, 1986

[33]   Chandler JW, Stabile KJ, Pfaeffle HJ, Li ZM, Woo SL, Tomaino MM: Anatomic parameters for planning of interosseous ligament reconstruction using computer-assisted techniques. J Hand Surg Am 28:111-116, 2003

[34]   Schneiderman G, Meldrum RD, Bloebaum RD, Tarr R, Sarmiento A: The interosseous membrane of the forearm: structure and its role in Galeazzi fractures. J Trauma 35:879-885, 1993

[35]   McGinley JC, Heller JE, Fertala A, Gaughan JP, Kozin SH: Biochemical composition and histologic structure of the forearm interosseous membrane. J Hand Surg Am 28:503-510, 2003

[36]   Noda K, Goto A, Murase T, Sugamoto K, Yoshikawa H, Moritomo H: Interosseous membrane of the forearm: an anatomical study of ligament attachment locations. J Hand Surg Am 34:415-422, 2009

[37]   Skahen JR, III, Palmer AK, Werner FW, Fortino MD: The interosseous membrane of the forearm: anatomy and function. J Hand Surg Am 22:981-985, 1997

[38]   Maitrise-orthop. Elbow Ligaments. 2010.

Ref Type: Internet Communication

[39]   Callaway GH, Field LD, Deng XH, Torzilli PA, O'Brien SJ, Altchek DW, Warren RF: Biomechanical evaluation of the medial collateral ligament of the elbow. J Bone Joint Surg Am 79:1223-1231, 1997

[40]   Armstrong AD, Ferreira LM, Dunning CE, Johnson JA, King GJ: The medial collateral ligament of the elbow is not isometric: an in vitro biomechanical study. Am J Sports Med 32:85-90, 2004

[41]   Moritomo H, Murase T, Arimitsu S, Oka K, Yoshikawa H, Sugamoto K: The in vivo isometric point of the lateral ligament of the elbow. J Bone Joint Surg Am 89:2011-2017, 2007

[42]   Safran MR, McGarry MH, Shin S, Han S, Lee TQ: Effects of elbow flexion and forearm rotation on valgus laxity of the elbow. J Bone Joint Surg Am 87:2065-2074, 2005

[43]   An KN: Muscle across the Elbow Joint: a Biomechanical analysis. Journal of Biomechanics 14:659, 1981

[44]   Magee DJ: Orthopedic Physical Assessment. W.B. Saunders, Philadelphia, 1992

[45]   Tanaka S.An K.N., Morrey B.F.: Kinematics and laxity of ulnohumeral joint under varus-valgus stress. Journal of Musculoskeletal Research 2:45-54, 1998

[46]   London JT: Kinematics of the elbow. J Bone Joint Surg Am 63:529-535, 1981

[47]   Deland JT, Garg A, Walker PS: Biomechanical basis for elbow hinge-distractor design. Clin Orthop Relat Res303-312, 1987

[48]   Bottlang M, Madey SM, Steyers CM, Marsh JL, Brown TD: Assessment of elbow joint kinematics in passive motion by electromagnetic motion tracking. J Orthop Res 18:195-202, 2000

[49]   Ericson A, Stark A, Arndt A: Variation in the position of the elbow flexion axis after total joint replacement with three different prostheses. J Shoulder Elbow Surg 17:760-767, 2008

[50]   Stokdijk M, Meskers CG, Veeger HE, de Boer YA, Rozing PM: Determination of the optimal elbow axis for evaluation of placement of prostheses. Clin Biomech (Bristol , Avon) 14:177-184, 1999

[51]   Hollister AM, Gellman H, Waters RL: The relationship of the interosseous membrane to the axis of rotation of the forearm. Clin Orthop Relat Res272-276, 1994

[52]   Epner RA, Bowers WH, Guilford WB: Ulnar variance--the effect of wrist positioning and roentgen filming technique. J Hand Surg Am 7:298-305, 1982

[53]   af Ekenstam F, Hagert CG: The distal radio ulnar joint. The influence of geometry and ligament on simulated Colles' fracture. An experimental study. Scand J Plast Reconstr Surg 19:27-31, 1985

[54]   Galik K, Baratz ME, Butler AL, Dougherty J, Cohen MS, Miller MC: The effect of the annular ligament on kinematics of the radial head. J Hand Surg Am 32:1218-1224, 2007

[55]   Pfaeffle HJ, Fischer KJ, Manson TT, Tomaino MM, Woo SL, Herndon JH: Role of the forearm interosseous ligament: is it more than just longitudinal load transfer? J Hand Surg Am 25:683-688, 2000

[56]   Stabile KJ, Pfaeffle J, Weiss JA, Fischer K, Tomaino MM: Bi-directional mechanical properties of the human forearm interosseous ligament. J Orthop Res 22:607-612, 2004

[57]   Rabinowitz RS, Light TR, Havey RM, Gourineni P, Patwardhan AG, Sartori MJ, Vrbos L: The role of the interosseous membrane and triangular fibrocartilage complex in forearm stability. J Hand Surg Am 19:385-393, 1994

[58]   Murray PM: Diagnosis and treatment of longitudinal instability of the forearm. Tech Hand Up Extrem Surg 9:29-34, 2005

[59]   DeFrate LE, Li G, Zayontz SJ, Herndon JH: A minimally invasive method for the determination of force in the interosseous ligament. Clin Biomech (Bristol , Avon) 16:895-900, 2001

[60]   Gabriel MT, Pfaeffle HJ, Stabile KJ, Tomaino MM, Fischer KJ: Passive strain distribution in the interosseous ligament of the forearm: implications for injury reconstruction. J Hand Surg Am 29:293-298, 2004

[61]   Pfaeffle HJ, Fischer KJ, Srinivasa A, Manson T, Woo SL, Tomaino M: A model of stress and strain in the interosseous ligament of the forearm based on fiber network theory. J Biomech Eng 128:725-732, 2006

[62]   Manson TT, Pfaeffle HJ, Herdon JH, Tomaino MM, Fischer KJ: Forearm rotation alters interosseous ligament strain distribution. J Hand Surg Am 25:1058-1063, 2000

[63]   Watanabe H, Berger RA, Berglund LJ, Zobitz ME, An KN: Contribution of the interosseous membrane to distal radioulnar joint constraint. J Hand Surg Am 30:1164-1171, 2005

[64]   Kihara H, Short WH, Werner FW, Fortino MD, Palmer AK: The stabilizing mechanism of the distal radioulnar joint during pronation and supination. J Hand Surg Am 20:930-936, 1995

[65]   Li ZM, Kuxhaus L, Fisk JA, Christophel TH: Coupling between wrist flexion-extension and radial-ulnar deviation. Clin Biomech (Bristol , Avon) 20:177-183, 2005

[66]   Short WH, Palmer AK, Werner FW, Murphy DJ: A biomechanical study of distal radial fractures. J Hand Surg Am 12:529-534, 1987

[67]   Werner FW, Palmer AK, Fortino MD, Short WH: Force transmission through the distal ulna: effect of ulnar variance, lunate fossa angulation, and radial and palmar tilt of the distal radius. J Hand Surg Am 17:423-428, 1992

[68]   Birkbeck DP, Failla JM, Hoshaw SJ, Fyhrie DP, Schaffler M: The interosseous membrane affects load distribution in the forearm. J Hand Surg Am 22:975-980, 1997

[69] Shepard MF, Markolf KL, Dunbar AM: Effects of radial head excision and distal radial shortening on load-sharing in cadaver forearms. J Bone Joint Surg Am 83-A:92-100, 2001

[70] Markolf KL, Lamey D, Yang S, Meals R, Hotchkiss R: Radioulnar load-sharing in the forearm. A study in cadavera. J Bone Joint Surg Am 80:879-888, 1998

[71] Chadwick EK, Nicol AC: Elbow and wrist joint contact forces during occupational pick and place activities. J Biomech 33:591-600, 2000

[72] Amis AA, Dowson D, Wright V: Elbow joint force predictions for some strenuous isometric actions. J Biomech 13:765-775, 1980

[73] Nicol AC. Elbow Joint Prosthesis Design: Biomechanical aspects. 1977.

Ref Type: Thesis/Dissertation

[74] An KN, Kwak BM, Chao EY, Morrey BF: Determination of muscle and joint forces: a new technique to solve the indeterminate problem. J Biomech Eng 106:364-367, 1984

[75] Brockman EP: Two Cases of Disability at the Wrist-joint following Excision of the Head of the Radius. Proc R Soc Med 24:904-905, 1931

[76] Curr JFCWA: Dislocation of the inferior radio-ulnar joint. British Journal of Surgery 34:74-77, 1946

[77] Essex-Lopresti P: Fractures of the radial head with distal radio-ulnar dislocation; report of two cases. J Bone Joint Surg Br 33B:244-247, 1951

[78] Reckling FW, Peltier LF: Riccardo Galeazzi and Galeazzi's Fracture. Surgery 58:453-459, 1965

[79] Auyeung J, Broome G: The Essex-Lopresti lesion: a variant with a bony distal radioulnar joint injury. J Hand Surg Br 31:206-207, 2006

[80] Leung YF, Ip SP, Ip WY, Kam WL, Wai YL: The crisscross injury mechanism in forearm injuries. Arch Orthop Trauma Surg 125:298-303, 2005

[81] Rozental TD, Beredjiklian PK, Bozentka DJ: Longitudinal radioulnar dissociation. J Am Acad Orthop Surg 11:68-73, 2003

[82] Jungbluth P, Frangen TM, Muhr G, Kalicke T: A primarily overlooked and incorrectly treated Essex-Lopresti injury: what can this lead to? Arch Orthop Trauma Surg 128:89-95, 2008

[83]   Chloros GD, Wiesler ER, Stabile KJ, Papadonikolakis A, Ruch DS, Kuzma GR: Reconstruction of essex-lopresti injury of the forearm: technical note. J Hand Surg Am 33:124-130, 2008

[84]   Harrington IJ, Sekyi-Otu A, Barrington TW, Evans DC, Tuli V: The functional outcome with metallic radial head implants in the treatment of unstable elbow fractures: a long-term review. J Trauma 50:46-52, 2001

[85]   Morrey B.F.: Radial Head Fracture. pp. 341-364. In Morrey B.F. (ed): The elbow and its disorders. W.B. Saunders; Philadelphia, 2001

[86]   Mason ML: Some observations on fractures of the radial head with a review of one hundred cases. British Journal of Surgery 42:123-132, 1954

[87]   King GJ, Evans DC, Kellam JF: Open reduction and internal fixation of radial head fractures. J Orthop Trauma 5:21-28, 1991

[88]   Davidson PA, Moseley JB, Jr., Tullos HS: Radial head fracture. A potentially complex injury. Clin Orthop Relat Res224-230, 1993

[89]   King GJW: Fractures of the Head of the Radius. pp. 845-887. In Green DPHRNPWCWSW (ed): Green's Operative Hand Surgery. Elsevier; Philadelphia, 2005

[90]   Ikeda M, Sugiyama K, Kang C, Takagaki T, Oka Y: Comminuted fractures of the radial head. Comparison of resection and internal fixation. J Bone Joint Surg Am 87:76-84, 2005

[91]   Hausmann JT, Vekszler G, Breitenseher M, Braunsteiner T, Vecsei V, Gabler C: Mason type-I radial head fractures and interosseous membrane lesions--a prospective study. J Trauma 66:457-461, 2009

[92]   Markolf KL, Tejwani SG, O'Neil G, Benhaim P: Load-sharing at the wrist following radial head replacement with a metal implant. A cadaveric study. J Bone Joint Surg Am 86-A:1023-1030, 2004

[93]   Van Glabbeek F, van Riet RP, Baumfeld JA, Neale PG, O'Driscoll SW, Morrey BF, An KN: Detrimental effects of overstuffing or understuffing with a radial head replacement in the medial collateral-ligament deficient elbow. J Bone Joint Surg Am 86-A:2629-2635, 2004

[94]   Van Glabbeek F, van Riet RP, Baumfeld JA, Neale PG, O'Driscoll SW, Morrey BF, An KN: The kinematic importance of radial neck length in radial head replacement. Med Eng Phys 27:336-342, 2005

Chapter 2

A Novel Forearm Simulator: Design and Validation

Overview: *To enable testing of the biomechanics of the forearm, a unique simulator was designed to analyze clinically meaningful loading conditions. This chapter outlines the design rationale as well as describes the features of the forearm simulator. Validation testing of the simulator and the outcome measurement tools are also reported.*

Publication: *This work has not been submitted for publication.*

2.1 Introduction

As described in Chapter 1, the forearm is a complex articular unit. Current simulators designed for benchtop testing employ denuded forearms(1), conduct osteotomies of the humerus (2) or radius and ulna (3) (4) (5) (6), or test aspects of the forearm (such as the radiocapitellar joint) in isolation (7). Many systems apply significant constraint to the upper extremity during testing (8) (9). The limitations of these systems and the desire to test the forearm as a unit for a variety of clinically meaningful scenarios led to the creation of a forearm simulator.

This device was designed and built to allow testing of cadaveric specimens as close to physiologic loading conditions as possible (Fig 2.1, App 1). Design parameters were selected to allow testing in a variety of biomechanical scenarios involving the elbow, forearm or wrist. The simulator required the ability to restrict or enable motion in three dimensions of translation and rotation of each of the rigid bodies of the radius, ulna and humerus. The ability to precisely control the direction, magnitude and rate of axial load application to the hand as well as passively rotate the forearm under position or torque control was important. Testing in different positions of elbow flexion and extension, as well as forearm pronation and supination, was also required for potential testing scenarios.
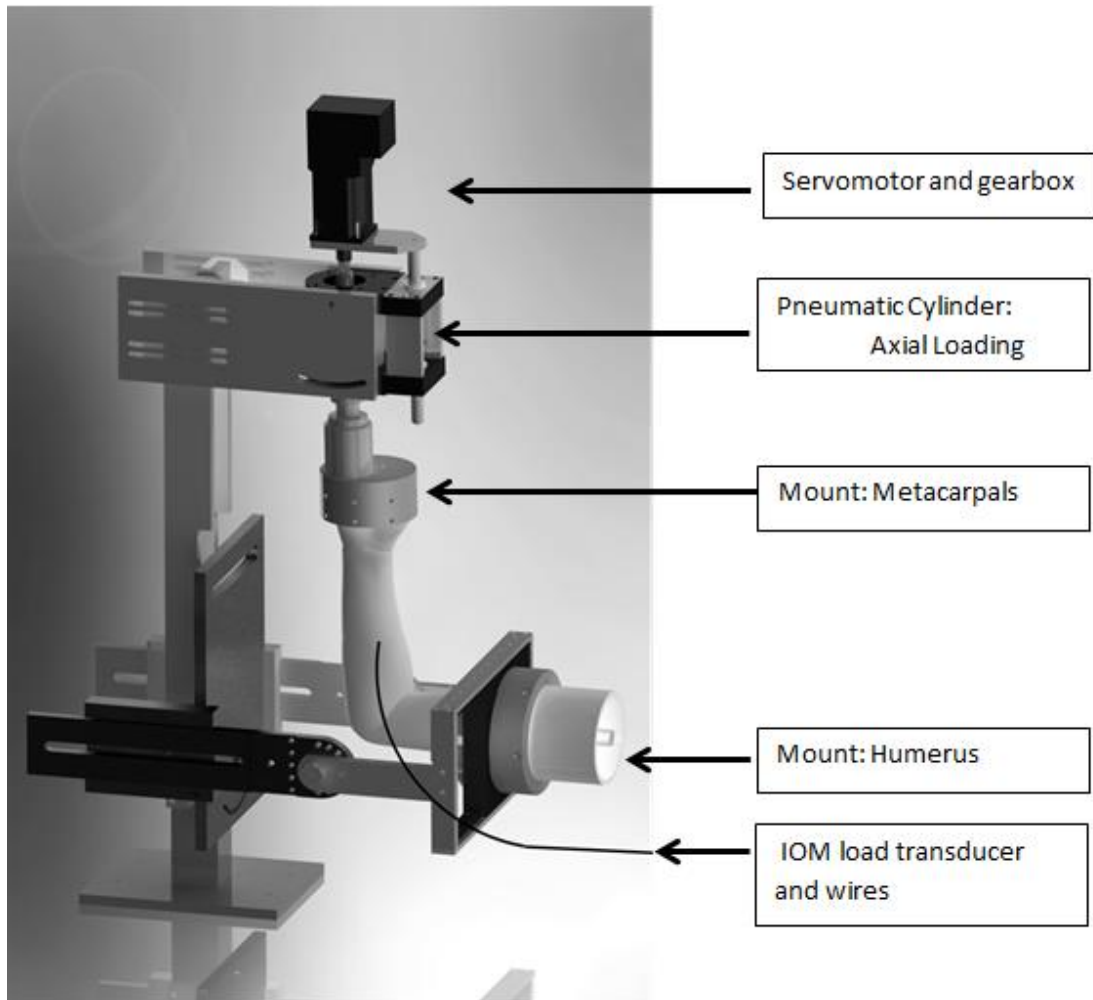
Figure 2.1: Isometric view of a computer based model of the simulator. Modelled is a simulated cadaveric arm, with the metacarpals and humerus potted for rigid fixation. The active units as well as the IOM load transducer are labelled.

2.2 Methods

2.2.1 Simulator Materials

Stainless steel type 316 (S31600) was selected for the testing device and fittings, due to machinability and high strength. The ability to resist corrosion in saline and cleaning products as well as ease of cleaning was also advantageous (13). Delrin was chosen for some components as it is inexpensive, had good strength and corrosion resistance, and is easy to machine. Delrin also has been shown to have minimal adhesion and static friction characteristics, allowing motion between components (14).

2.2.2 Degrees of Freedom

Normal activities involving the upper extremity involve forces transferred via the hand. These forces, and the reaction forces created by the muscles of the forearm, are transferred at the articulations of the forearm. To create a simulator capable of physiologic loading of the forearm, the most simplistic design would involve rigid fixation of the osseous bodies of the forearm, apply loads, and record soft tissue or joint reaction forces. However, this does not accurately represent the complexity of the upper extremity, and applies unwanted internal forces as a result of constraint. The simulator was designed to have multiple degrees of freedom (DOF) to allow minimal constraint, precise load positioning, and allowance for a variety of specimen sizes. Where possible, each DOF had the ability to be constrained or not. A total of 17 DOF was provided, seven at the wrist and seven at the elbow with the remaining 3 DOF to allow adjustability at the ulnar attachment when used (Fig 2.2(A)). Slots with bolts (Fig 2.2(B)) to allow

(A)
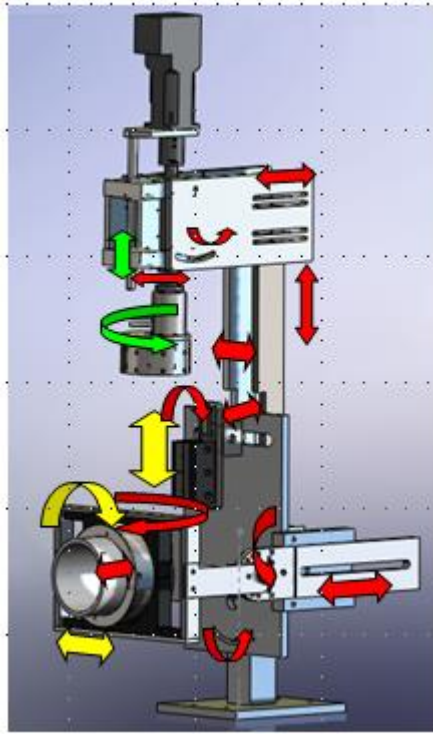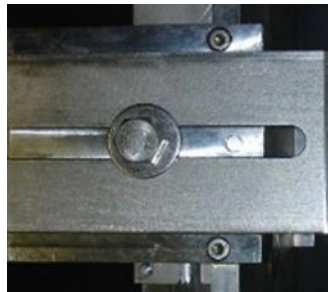
(B)   (C)
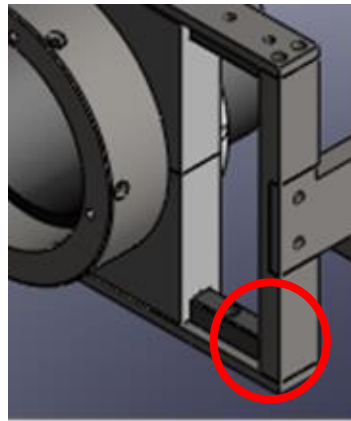
Figure 2.2: The degrees of freedom potentiated by the simulator; a total of 17 included in the final design (A). Detail image demonstrating bolts within a slot that allowed translation (B). Delrin tongue and groove construct (circled) at the humerus mount (C).

translation or pivoting were used predominantly on the upper aspect of the simulator, where the load was applied to the metacarpals. This construct was preferred to allow adjustability as well as strength when the final position of the arm was selected. In contrast, the ulna and humerus mounts were selected to optimize mobility, with secondary goals of minimizing constraint. To allow the humerus to more precisely align with the loading of the forearm as well as prevent abnormal loading at the elbow due to constraint, the humerus was allowed to horizontally translate as well as rotate. Motion in translation was enabled by mounting the humerus mount on lubricated Delrin rails in a tongue and groove pattern. Similarly, rotation was enabled by slotting the circumference of the cylindrical humerus mount and fitting this slot into a lubricated Delrin collar for a circular tongue and groove construct (Fig 2.2(C)). Lubrication was utilized in the tongue and groove constructs to decrease friction, and allow the specimen to move to a position of lower reactionary forces; thereby decreasing the constraint and associated forces within the specimen.

The simulator has the capability to allow the ulna to be constrained to a fixed mount rather than including the humerus. Using a Delrin mount, the ulna's connection could be optimized for each specimen. If only partially constrained, this mount allowed translation by low friction roller track bearings as well as bolted mount points in slots to allow translation.

2.2.3 Pronation/Supination

Forearm rotation through pronation and supination was found on pilot tests to require less than 3 Nm of torque. To provide smooth motion in a highly controlled fashion, a servo motor was selected rather than a stepper motor or a pneumatic motor.

The Animatics SM2315DT servo motor (Moog Animatics ®, Santa Clara CA, USA) has

an incorporated amplifier and motion control system (App 2). This motor produces a

torque of 0.4 Nm, and rotates to a maximum revolutions per minute (RPM) of 4700. As

the output torque was too low a reduction gear ratio was employed.   The gearbox

selected was the Animatics single stage GH23P22 (App 2b). This provided a 22:1 gear

ratio to allow the servo motor to provide the design parameter outputs. Motor torque

multiplied by gear ratio provides an output torque of 8.8 Nm (22X0.4). The design safety

factor for torque is 2.5, and higher than the reported physiologic torque (10).

2.2.4   Axial Loading

Axial loads are transmitted through the forearm with upper extremity activity and

therefore were a critical aspect of creating a simulator. The capability of testing via

compression as well as distraction was a design criteria. Physiologic forces at the

articulations of the forearm are high (11). However, preliminary testing necessitated

testing lower than 200 N as testing above 200 N resulted in mid-carpal instability during

pilot testing. An axial load of 160 N was selected as other investigators have reported

that axial loads of over 200 N did not affect the load sharing results (12). Precise control

of a constant load while the point of load application translates was a design necessity.

The ability of the device to translate was required due to the characteristics of the forearm

loading, the relative change in radial length during forearm rotation while other rigid

bodies of the upper extremity remained fixed, interspecimen variability, as well as the

ease of mounting each specimen. Axial loading was applied by a pneumatic actuator

(Model FOD-094-S, Bimba®, University Park, IL, USA) (App 3). This specific actuator

was selected as this cylinder features a double acting, double ended rod. The double

ended feature of a pneumatic cylinder allowed for protrusion of the central rod of the

cylinder from both ends of the cylinder, and is a single component. This feature allowed

rotational forces to be applied and transmitted independent of axial loads. The double

acting feature of the actuator allowed both compressive and distraction loads to be

applied. To apply an appropriate load, a 1-1/16" diameter cylinder was selected. Power

Factor is defined as the output force produced by the pneumatic cylinder as impacted by

the input pressure with a fixed cross sectional area of the inside of the cylinder. Given

that the power factor for a 1-1/16" cylinder is 0.88, and the available pneumatic source

pressure was 100 psi, the actuator can produce 400 N of force. This represents a 2.5 X

safety factor of design capability to testing requirements. The length of travel of this

cylinder is 101 mm to allow both for appropriate loading of the specimen, as well as

allow ease of mounting.

To allow application of a constant load with precision, a load cell (Futek® Model MBA

600, Irvine, CA) was interfaced between the load application and the specimen (App 4).

This also allowed measurement of the reaction forces of the forearm to the applied forces.

A closed-loop feedback with a custom software controller allowed precise maintenance

of the desired load applied. The manufacturer's calibration constants and National

Institute of Standards and Technology (NIST) calibration certificate were utilized.

2.2.5 Torque Measurement

Reaction forces to rotation were measured using a load cell (Futek® Model MBA 600,

Irvine, CA)(App 4) that was rigidly fixed to the servomotor which applied the rotational

torque as well as the load to the metacarpals. This torque was recorded in a continuous

manner. Again, the manufacturer's calibration constants and NIST calibration certificate were utilized.

2.2.6 IOM Load Cell

Minimal dissection of the IOM while recording the forces was important. To do so, a custom load cell was constructed. A pair of strain gauges (Vishay Micro-Measurements®, 120 Ω, 90° rosette, Raleigh, NC) were affixed to a strip of spring steel 9.5 x6.5 x 0.32 mm (Fig. 2.3(A)). Utilizing a three point bending concept, the load cell was woven through the fibers of the IOM (Fig 2.3(B)). The load cell was calibrated by weaving it through the fibers of a synthetic material and utilizing hanging weights. Using IOM tissue for calibration was not found to be technically possible due to the obliquity of the fibers to the bone as well as the friable nature of the tissue. Temperature was controlled and maintained throughout testing.

2.2.7 Radiocapitellar Joint Pressure

To determine the contact area and pressure at the radiocapitellar joint, a thin rectangular film sensor was utilized (K-Scan system, Model 4201, I-Scan 5.761 software, Tekscan®, South Boston, MA)(App 5). This sensor was larger than required for the radiocapitellar joint space. Initial attempts to trim the sensor to fit the specimen's intra-articular space caused early failure and a lack of reliability of the device. Attempts to provide a watertight seal to the cut edges were not successful. Therefore, the sensor was marked to produce consistent positioning of the sensor as well as any deformation points. The peaks of contact pressure and area at points of deformation were manually removed when testing had been completed.

(A)

(B)

Optical Tracker Mount

Central Band of IOM

Strain gauges

Ulna
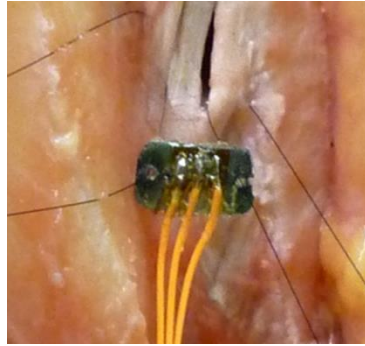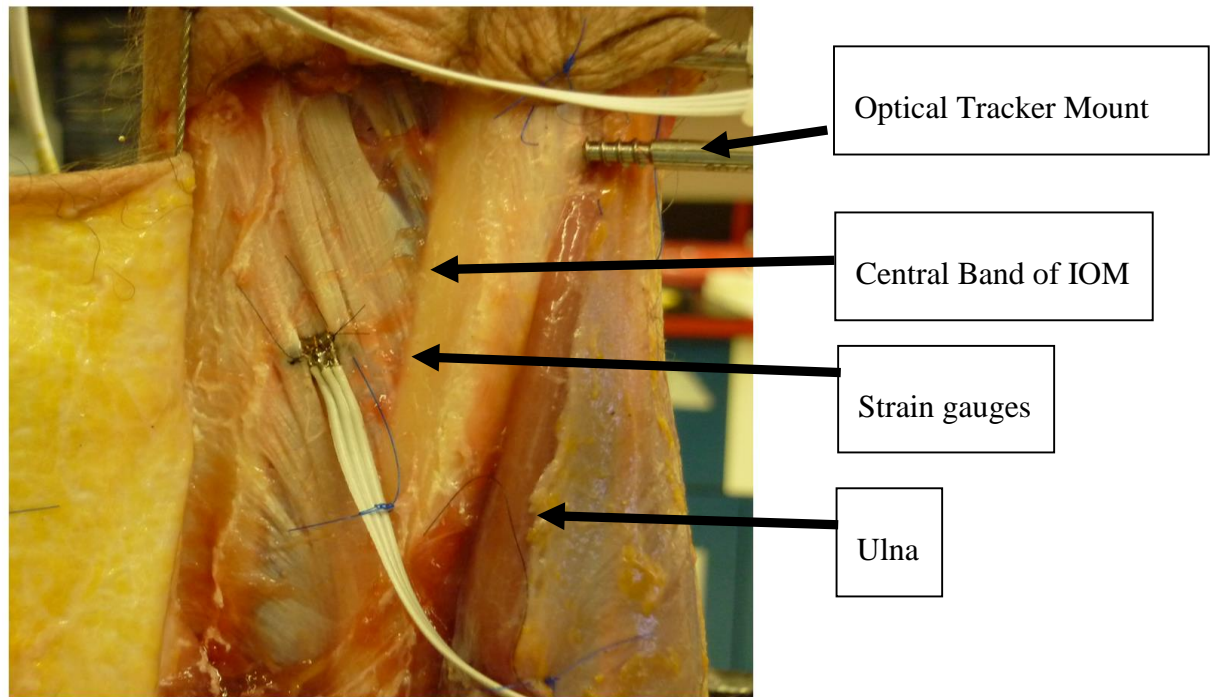
Figure 2.3: Custom load created to allow direct measurement of IOM tension during pronation-supination testing of the forearm. (A) Pair of strain gauges attached to a strip of spring steel. (B) Woven through the fibers of the IOM, and sutured to the IOM tissue

2.2.8   Motion Measurement

The ability to track the motion of each rigid body of the upper extremity (ulna, radius and humerus) during testing was also selected as an important design feature. To do so, the precision of optical tracking systems was selected, and the load bearing aspects of the simulator were designed to allow open access to the specimen to facilitate continuous tracking (App 6 (A)). Also, the simulator was painted a flat black to decrease the reflection of infrared beams. As part of the validation of this system, active (signals sent to recording device) and passive (central device emits signal and records reflected signal to determine position) trackers were affixed to the radius, ulna and humerus using an external fixator (App 6(B)). Pilot testing indicated that active tracking was possible through a complete range of pronation and supination.

2.2.9   Reproducibility/Repeatability Testing

Expertise using the simulator was gained in preliminary testing using six specimens. Reproducibility and repeatability testing was done prior to proceeding with the final protocol using a single thawed cadaveric upper extremity specimen (68 yo female). The fingers were disarticulated at the metacarpo-phalangeal joints, and the thumb at the carpo-metacarpal joint. The metacarpals were stripped of all soft tissues, leaving the tendinous insertions at the bases and the joint capsules intact. The humeral shaft was denuded starting 8 cm above the elbow joint.   A dorsal trapdoor was made using a Thompson approach to access the central band of the IOM, and the extensor digitorum communis was resected over the central band of the IOM. The remainder of the soft tissue was retained, and retracted toward the ulna to expose the IOM for 10 cm directly

overlying the central portion of the IOM. Two 8 mm long parallel slits were made 4 mm apart in the central band parallel to the IOM fibers. The strain gauge was woven into the central band of the IOM using two parallel slits 4 mm apart and secured using 5.0 silk suture (Ethicon, San Antonio, TX).

After positioning the wrist in neutral in all planes and the third metacarpal in line with the direction of the applied loads, the metacarpals were transversely pinned in position. The metacarpals were then potted using bone cement. The humerus was also potted using bone cement. The forearm was taken through a range of motion of pronation and supination and the elbow through a range of flexion and extension to ensure minimal resistance to motion as well as recording the range of rotation possible. This range of pronation and supination was then precisely repeated by the simulator throughout testing. Two kilogram weights were sutured to the tendons of the brachialis, biceps and four kilograms to the triceps tendons using No. 2 Ethibond® (Ethicon, San Antonio, TX), with maintenance of the direction of pull using adjustable pulleys.

The common extensor tendon and the underlying annular ligament were split to provide a direct lateral approach to the radial head. Although a small portion of the radial collateral ligament was released off the humerus to provide adequate exposure, the humeral and ulnar attachments of the lateral ulnar collateral ligament were preserved. The annular ligament, radial collateral ligament and common extensor tendon split were repaired in layers using interrupted No. 2 Ethibond® sutures (Ethicon, San Antonio, TX) at each stage of the testing protocol.

Reproducibility and repeatability testing was done with the native radial head under active motion. Each arm was tested through a full range of pronation and supination for three cycles to condition the specimen. All testing was done at 240 N of axial load, and positions of elbow flexion of 0, 45 and 90 degrees was done to ensure that reproducibility and repeatability was not effected by position. For repeatability testing, the IOM tension was measured continuously for a total of five cycles. Between each cycle, the test was halted, and the axial load removed. The load was re-applied, and another cycle of pronation and supination was conducted. To test for reproducibility, the specimen was removed from the forearm simulator after the first sequence of repeatability testing. Although it was not possible to remove the cement around the bone without damaging the metacarpals, the mounting points were disconnected from the simulator. The metacarpal and humeral pots were then remounted. The test sequence above was then reapplied. Repeatability testing was conducted once more, with the same outcomes being measured.

2.3 Results

Repeatability of the IOM load sensor was good with a Pearson correlation coefficient of greater than 0.9 and a mean standard deviation of <0.1. Assessment of the load sensor calibration ex-vivo revealed a high Pearson correlation of 0.98. Contact area had good repeatability, with a Pearson correlation of greater than >0.5. However, contact pressure had only a medium Pearson correlation suggesting these measurements were less reliable (r=0.4). Repeatability of torque outcomes using a Pearson correlation was found to be 0.95, with an average standard deviation of less than 0.1. Reproducibility testing

conducted revealed good correlation for torque measures (Pearson 0.85, mean standard deviation <0.1), with moderate correlation for the IOM testing (0.52).

2.4 Discussion

Design and construction of this novel forearm simulator was completed in an iterative fashion. Testing using the simulator demonstrated the ability to test with the soft tissues largely intact. The design was demonstrated to allow axial loads to be applied in a controlled fashion while testing during active forearm rotation. Continuous measurement of the IOM tension using a novel testing system was demonstrated to be possible with good repeatability and reproducibility. Quantifying IOM tension is important to understand load transfer within the forearm, and this system will allow for testing of clinically important scenarios. The clinical meaning of torque, the rotational resistance of the forearm to rotation, has not been fully delineated. However, it likely includes an aggregate effect of articular forces, and does provide another useful metric for understanding the biomechanics of the forearm. Validation testing demonstrated continuous measurement of forearm torque was possible with good repeatability and reproducibility. Radiocapitellar contact properties were successfully quantified as well. The repeatability and reproducibility measures were not as strong as other outcomes measured. The radiocapitellar joint areas had good repeatability, however, the contact pressure measures were less reliable. The reasons for this are potentially multi-factorial. Physical deformation of the sensor due to the limitations of space within the radiocapitellar joint was necessary. This required manual interpretation and removal of these areas of deformation in contact force and area outcomes. Although carefully

marked to attempt to place the sensor in the same position each time, re-insertion in the exact same position may not have been possible. Use of a custom sized sensor would strengthen future testing.

The design and reproducibility and repeatability testing of the simulator did have some weaknesses. Tekscan was used to measure the articular contact area and pressure and as outlined above, validation testing demonstrated precision limitations of the Tekscan outcomes, particularly contact pressure. Although preliminary testing demonstrated that testing while recording forearm kinematics with the optical tracking system was possible, outcomes were not quantified or validated. Under higher axial loads, mid-carpal instability occurred, limiting the simulator's ability to test more provocative loading magnitudes. The simulator was designed to have multiple degrees of freedom with the ability to selectively constrain depending on the testing protocol. However, there was likely some frictional resistance in these planes of motion, particularly under axial loads, which were not quantified.

Strengths of this simulator are that it allows testing in a physiologically relevant way while allowing measurement of the IOM loading conditions as well as radiocapitellar joint contact mechanics. A variety of clinically important questions can be tested that relate to the wrist, elbow or forearm. Measurement of multiple outcomes while being minimally invasive allows clinically important data to be collected. Unique measurement tools and the means of load application allow testing of specific forearm properties with minimal soft tissue dissection using this forearm simulator.

2.5 Conclusions

A forearm simulator with multiple degrees of freedom, loading and measurement tools was designed, built, and tested for repeatability and reproducibility. The potential to enable multiple clinically relevant testing scenarios was achieved.

2.6 References

1. Gabriel M, Pfaeffle HJ, Stabile KJ, Tomaino MM, Fischer KJ. Passive Strain Distribution in the Interosseous Ligament of the forearm: implications for injury reconstruction. Journal of Hand Surgery, 2003:29(2); 293-298.

2. Rabinowitz RS, Light TR, Havey RM, Gourineni P, Patwardhan AG, Sartori MJ, Vrbos L. The Role of the Interosseous Membrane and Triangular Fibrocartilage Complex in Forearm Stability. Journal of Hand Surgery, 1994:19(3); 385-393.

3. Chloros GD, Wiesler ER, Stabile KJ, Papadonikolakis A, Ruch DS, Kuzma GR. Reconstruction of Essex-Lopresti Injury of the Forearm: Technical Note. 2008, Journal of Hand Surgery (Am), Vol. 33, pp. 124-30.

4. Manson TT, Pfaeffle HJ, Herdon JH, Tomaino MM, Fischer KJ. Forearm Rotation Alters Interosseous Ligament Strain Distribution. Journal of Hand Surgery, 2000:25(6); 1058-1063.

5. Markolf KL, Lamey D, Yang S, Meals R, Hotchkiss R. Radioulnar Load Sharing in the Forearm: A Study in Cadavera. Journal of Bone and Joint Surgery, 1998:80(6): 879-888.

6. Shepard, M, Markolf, K and Dunbar, A. Effects of Radial Head Excision and Distal Radial Shortening on Load-Sharing in Cadaver Forearms. The Journal of Bone and Joint Surgery, 2001:80(6); 93-100.

7. Liew VS, Cooper IC, Ferreira LM, Johnson JA, King GJ. The Effect of Metallic Radial Head Arthroplasty on Radiocapitellar Joint Contact Area. Clin Biomech 2003:18(2);115-8.

8. Watanabe H, Berger RA, Berglund LJ, Zobitz ME, An KN. Contribution of the Interosseous Membrane to Distal Radioulnar Joint Constraint. Journal of Hand Surgery (Am), 2005: 30; 1164-71.

9. Shaaban H, Giakas G, Bolton M, Williams R, Wicks P, Scheker LR, Lees VC. Contact area inside the distal radioulnar joint: effect of axial loading and position of the forearm. Clinical Biomechanics, 2007:22; 313-8.

10. Gordon KD, Pardo RD, Johnson JA, King GJW, Miller TA. Electromyographic Activity and Strength during Maximum Isometric Pronation and Supination Efforts in Healthy Adults. Journal of Orthopaedic Research, 2004:22;208-13.

11. Chadwick, E and Nicol, A. Elbow and Wrist Joint Contact Forces during Occupational Pick and Place Activities. Journal of Biomechanics, 2000:591-600.

12. Markolf KL, Dunbar AM, Hannani K. Mechanisms of Load Transfer in the Cadaver Forearm: Role of the Interosseous Membrane. Journal of Hand Surgery (Am), 2000:25;674-82.

13. The A to Z of Materials. [Online] [Cited: June 25, 2013.] www.azom.com/article.aspx?ArticleID=2382.

14. Dupont Plastics. [Online] Dupont. [Cited: June 20, 2013.] http://plastics.dupont.com/plastics/pdflit/europe/delrin/DELLWLFe.pdf.

Chapter 3

Effect of Radial Head Excision and Arthroplasty on Interosseous Membrane Tension

Overview: *Radial head excision as well as radial head arthroplasty have been described as a treatment for complex radial head fractures. However, how each treatment changes load transfer within the forearm is not understood. This chapter compares interosseous membrane tension after both radial head excision and arthroplasty to the native radial head state under static and dynamic loading conditions.*

Publication: *Lanting BA, Ferreira LM, Johnson JA, Athwal GS, King GJ. The effect of excision of the radial head and metallic radial head replacement on the tension in the interosseous membrane. Bone Joint J. 2013 Oct; 95-B (10): 1383-7*

3.1 Introduction

Radial head fractures are common, with the majority being minimally displaced and successfully treated non-operatively [1]. Surgical management may be required for more displaced fractures. Open reduction and internal fixation, while successful for simple displaced fractures, has been less reliable when treating fragmented and osteopenic fractures due to a higher incidence of complications [2]. Treatment of comminuted radial head fractures may include excision or arthroplasty; the optimal treatment is unknown [3].

In long-term studies, radial head excision has been shown to have satisfactory functional outcomes in spite of a high incidence of osteoarthritic changes [4] and concerns with proximal radial migration [5]. Other literature supports the effectiveness of metallic radial head arthroplasty [6]. No randomized studies have compared the outcomes of radial head excision and arthroplasty. Soft tissue injuries of the elbow are common with

comminuted radial head fractures, [7] as interosseous membrane (IOM) damage has been demonstrated to be common in even relatively low energy fractures [8].

The purpose of this study was to examine the effect of radial head excision and arthroplasty on forearm biomechanics as compared to the native radial head. The magnitude of IOM tension, position of the maximum IOM tension, and characterization of the IOM tension profile were examined.

3.2 Materials and Methods

An in-vitro forearm motion simulator, as described in Chapter 2, was developed in an effort to recreate the biomechanical forces transmitted through the forearm in a physiologic manner. The simulator (Fig. 3.1) was designed to produce axial loading of the forearm while simultaneously generating automated passive pronation and supination. This device allowed unconstrained motion through the carpus, radius, ulna and elbow. The humeral mount permitted medial-lateral translation, varus-valgus angulation, and axial rotation. Multiple degrees of freedom were incorporated into the simulator to ensure adjustability for each specimen, and to allow forearm loading with minimal constraint. The metacarpals were potted in bone cement such that the third metacarpal was in-line with the axis of the applied load, and the forearm was aligned with the applied load prior to potting the humerus.

Axial loading was applied through the metacarpals by a pneumatic actuator (Model FOD-094-S, Bimba®, University Park, IL) and governed by a custom software controller using closed-loop feedback from a load cell (Futek® Model MBA 600, Irvine, CA). Forearm pronation and supination motion was driven by a servomotor (Model SM2315-DT, Animatics®, Santa Clara, CA), with a cycle of rotation from pronation to supination and back to pronation in six seconds. To measure tension in the interosseous membrane (IOM), a custom load cell was constructed with a pair of strain gauges (Vishay Micro-Measurements®, 120 Ω, 90º rosette, Raleigh, NC) affixed to a strip of spring steel 9.5 x6.5 x 0.32 (Fig. 3.2). The load cell was woven over and under the IOM fibers, and this produced a bending axis via a three point loading construct. After calibration, the load cell was able to quantify IOM tension in real-time under kinematic loading conditions.
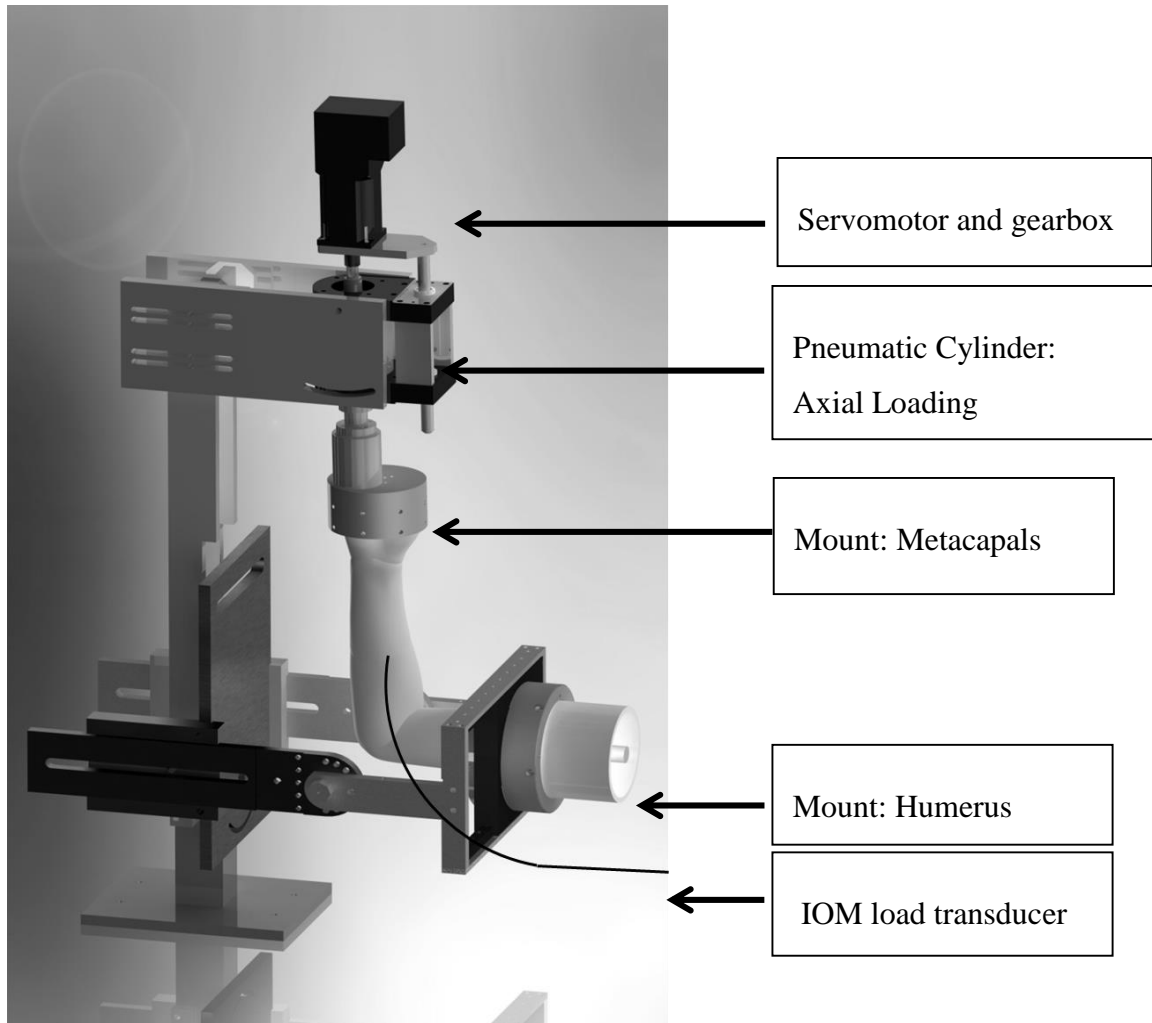
Figure 3.1 The dynamic forearm simulator, modeled with a specimen mounted in the metacarpal and humeral pots.
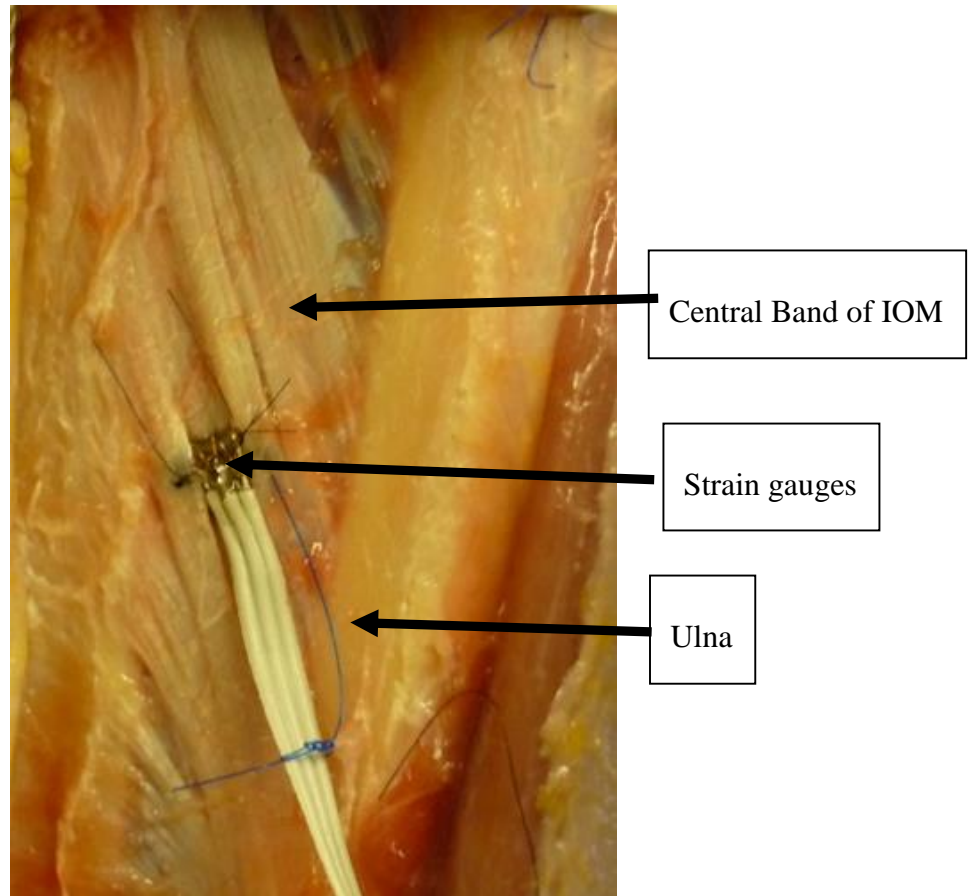
Figure 3.2 The load transducer, woven into the central band of the IOM

Six cadaveric specimens (mean age 65, range 52-72 yrs) were prepared for testing. The specimens were included only if there was no prior fracture or evidence of arthritis, based on pre-testing Computed Tomography (CT) scans. The arms were thawed at room temperature for 16 hours. The fingers were disarticulated at the metacarpo-phalangeal joints, and the metacarpals were stripped of all soft tissues. The thumb was disarticulated at the carpo-metacarpal joint. The tendinous insertions to the metacarpal bases were maintained, as were the joint capsules of the wrist and carpal bones. All soft tissue was stripped off the humeral shaft starting 8 cm above the elbow joint.   Via a Thompson approach, a volar trapdoor was made to access the central band of the IOM, hinging the soft tissue at the ulna. The extensor digitorum comminus was resected over the central band of the IOM. The remainder of the musculotendinous units were gently retracted to expose the IOM for a distance of 10 cm directly overlying the central portion of the IOM. The proximal and distal portions of the IOM were sectioned to isolate the central band. Two 8 mm long parallel slits were made 4 mm apart in the central band parallel to the IOM fibers. Both ends of the load sensing device were then inserted into the slits, thus weaving it into the central band of the IOM. Small holes at each end of the load cell were used to secure it to the IOM using 5.0 silk suture (Ethicon, San Antonio, TX) (Fig 3.2).

A Steinman pin was temporarily placed transversely through the metacarpals and the specimen was positioned with the wrist in neutral in all planes, and potted using bone cement with the third metacarpal in line with the applied loading vector. The elbow was flexed to 90°, and the forearm and carpus aligned with the applied axial load. The humerus was potted, and the limits of forearm rotation for each specimen were assessed manually and recorded by servomotor position feedback. These terminal ranges of motion were then precisely repeated throughout all trials. Static muscle forces across the elbow were simulated with weights by suturing cables to the tendons of the brachialis, biceps and triceps using No. 2 Ethibond® (Ethicon, San Antonio, TX). Two kg were applied to the brachialis and biceps brachii, and 4 kg to the triceps [9].   Muscle lines-of-action were maintained with an arrangement of adjustable pulleys.

A direct lateral approach to the radial head was performed by splitting the common extensor tendon and the underlying annular ligament. A small portion of the radial

collateral ligament was released off the humerus to provide adequate exposure to resect and replace the radial head, but the humeral and ulnar attachments of the lateral ulnar collateral ligament were preserved. A microsagittal saw was used to make the radial neck cut. The native radial head diameter and length was measured using calipers and the optimal radial head arthroplasty size was selected. The radial canal was hand reamed and a trial radial stem and head were inserted (Evolve®, Wright Medical Technology, Arlington, TN). The annular ligament, radial collateral ligament and common extensor tendon split were repaired in layers using interrupted No. 2 Ethibond® sutures (Ethicon, San Antonio, TX).

Both active motion and static testing were conducted. For the active series, each arm was tested through a full range of pronation and supination for three cycles for each radial head state at 160 N. IOM tension was measured continuously, with the third cycle used for data analysis. The arm was then tested statically in neutral rotation. The load was applied at a rate of 8 N/s to 160 N. The forearm was tested with the native radial head, with the radial head excised, and with the radial head replaced. The IOM tension recorded was plotted, and a line of best fit applied. The slope of this line of best fit was measured, and recorded as the rate of increase of IOM tension.

3.2.1 Statistical Methods

One and two-way ANOVA were utilized to calculate statistical significance, defined as $p<0.05$, for the dependent variable of IOM tension. Repeatability was assessed by determining linear dependence using the Pearson correlation coefficient of the IOM load sensor of sequential testing with the same test series.

3.3 Results

The system demonstrated good repeatability, with the IOM load sensor having a Pearson correlation coefficient of greater than 0.9, and a standard deviation of 0.7.

IOM tension increased after radial head excision during forearm rotation under a constant load, to almost double the values for the native or arthroplasty radial head states ($p=0.007$) (Fig. 3.3). There was no significant difference in IOM tension between the
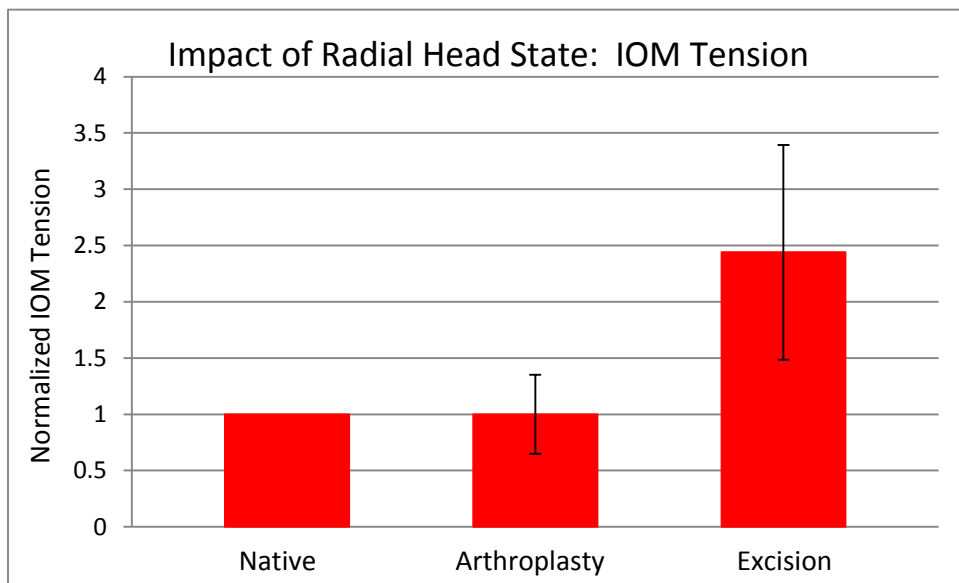
Figure 3.3 Maximum IOM tension in response to a constant (160N) axial load with dynamic forearm rotation with three radial head states: native, arthroplasty, excision. Normalized to the native radial head values.

native radial head and radial head arthroplasty states (p=0.09). Maximal IOM tension was measured in neutral rotation with both the native and replaced radial head. When the radial head was excised, maximal IOM tension occurred with the forearm in pronation.

Under dynamic axial loading, the rate of increase in IOM tension was more rapid when the radial head was excised than for the native or arthroplasty states (p=0.02), (Fig 4-representative specimen) as well as the average rate of increase for each specimen (Fig 5). When the radial head was excised, the rate of tension increase occurred at a higher rate than either the native or radial head arthroplasty states (p = 0.02). However, following radial head replacement, there was no difference in the rate of increase of IOM tension compared to the native radial head (p=0.78). The average rate of IOM tension increase was lower than the rate of applied axial load (Fig 4).
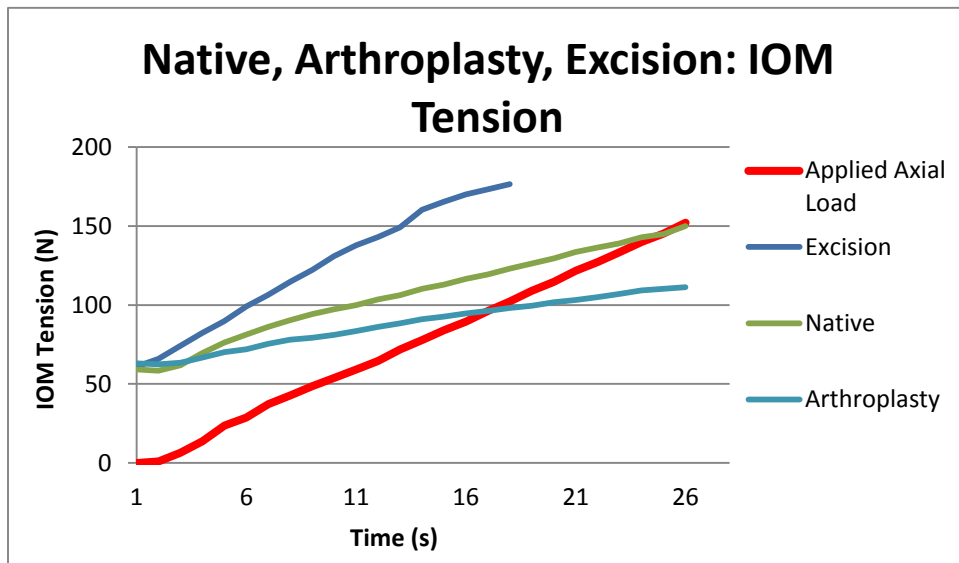
Figure 3.4 IOM response to axial loading under three radial head states: native, arthroplasty, excision in a static position under increasing axial loads for a single representative specimen
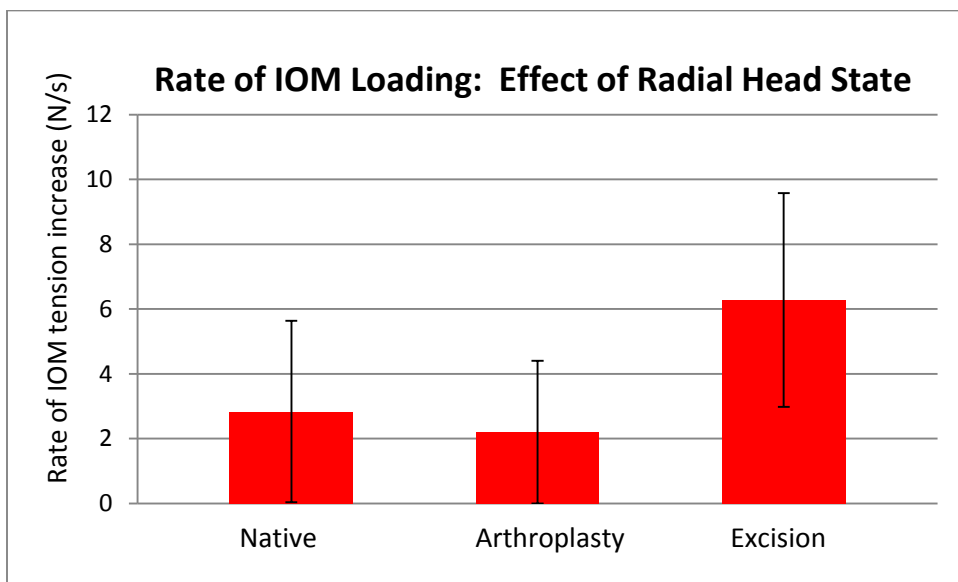
Figure 3.5 Rate of IOM response to axial loading under three radial head states: native, arthroplasty, and excision in a static position under increasing axial loads as calculated from the slope of the best line of fit to the measured IOM tension, error bars indicate one standard deviation.

3.4 Discussion

The forearm simulator permitted physiologic testing of the forearm in a repeatable way. This enabled us to quantify the effect of axial loading and radial head excision and arthroplasty on IOM tension. The axial loads applied in this study were higher than in previous reports [1] [10] [11] to reflect the higher loads that can occur physiologically [12].

Direct instrumentation of the IOM with a calibrated strain gauge-based load cell has advantages over calculated IOM tension. In most previous studies, the relationship between the IOM and radio-ulnar loading has been indirectly determined from strain gauges implanted in the osteotomized radius and ulna [13] [14] [15]. IOM tension has only been directly measured in one study, using an arthroscopically implantable force probe. However, although the IOM wasn't violated for measurement of the IOM tension, osteotomies of the radius and ulna were used, and no radial head arthroplasty group was included [13]. Thus, direct comparison to the current study is not possible.

The position of the greatest IOM tension has been found to occur in a variety of forearm rotations. Some literature describes the position of greatest IOM tension to be in neutral [16] [14] [17], or supination [10] [18]. Other studies report that the IOM is isometric [19]. In this study, the position of maximal IOM tension in an intact forearm was found to be in neutral. This was also found with the radial head arthroplasty. With the radial head excised, the IOM load was maximal in pronation; which is in keeping with other studies [16]. In pronation, the radius crosses over the ulna. If the radial head is excised, proximal control of the radio-ulnar relationship is lost, which may require greater IOM tension to maintain this relationship.

Excision of the radial head alters the radioulnar relationship; creating different IOM tensions than found in the intact or arthroplasty states. Excision of the radial head resulted in an increase in IOM tension; the average change was greater than double the values seen with the radial head intact or replaced (Fig 3.3).

It was found that the radial head state has an impact on soft tissue loading of the forearm. The observed increase in IOM tension found if the radial head is excised may lead to the potential for attritional failure over time. Also, the fact that the IOM tension is not changed when the radial head is replaced as compared to the native radial head is clinically important. This indicates that radial head arthroplasty may allow the forearm to maintain normal biomechanics and load transfer between the radius and ulna. If the IOM was damaged during trauma to the forearm that caused the radial head fracture, the IOM may be able to heal normally if the radial head is replaced. Given the challenges treating chronic longitudinal radioulnar dissociation [20], this potentially eliminates a significant clinical complication.

The ability to dynamically load the forearm and measure IOM forces has allowed the characterization of the IOM forces under a changing axial load. In a neutral position, there was no statistical difference in the increase in IOM tension between the native and radial head arthroplasty states. The absolute values of the IOM tension after radial head arthroplasty are lower in the single specimen displayed (3.4), but this may be due to a slight lengthening of the radial head compared to the native head. However, when the radial head was excised, the biomechanics of the forearm are changed. As a result, the amount of load the IOM transfers increased at a higher rate. The increased rate of IOM tension increase is intuitive, but has not been reported in the literature previously. The average rate of increase of IOM tension was less than the rate of applied axial load in all radial head states. The potential for load to be transferred via other soft tissue structures or differential rates of stress relaxation may explain this; however, it is unclear as to why this occurs. Also, the initial readings of IOM tension indicated a baseline tension of 50 N. This may be due to an introduction of tension to the IOM when the strain gauge is woven between the fibers, but may also be due to resting tension of the IOM.

The IOM response to the radial head state has clinical implications. Higher magnitudes of IOM tension under constant axial loads as well as greater increases in IOM tension under changing axial loads may impact patient outcomes both for short and long term scenarios. If treated with a radial head excision, rehabilitation should be protective of the IOM, with low force activities to allow associated soft tissue injuries of the forearm to

heal. This would include focusing on active pronation and supination exercises initially, with decreased emphasis on axial loading exercises. The patient should be counseled that permanent restrictions may be appropriate due to the potential for attritional damage with delayed radio-ulnar longitudinal drift [5]. If treated with a radial head arthroplasty, the forearm biomechanics are restored, so higher intensity rehabilitation can be re-instituted soon after surgery. Although there is clinical controversy about whether the IOM does heal, a correctly sized radial head would maintain the biomechanics of the forearm, and allow the potential for IOM healing. The patient potentially would be able to tolerate higher impact activities long term with a lower risk of attritional changes to the IOM.

This was an in-vitro cadaveric study with elderly specimens, which has inherent limitations. Whether the results of this study can be directly applied to younger patients' in-vivo remains to be confirmed. Associated LCL injuries were not modelled. Although proximal and distal sectioning of the IOM may be considered a weakness, it was done in recognition of the fact that the central band is the most important portion of the IOM [16], and that it is a discrete structure amenable to the novel measurement techniques used. The uncemented stem of the radial head replacement is the same as those used clinically. However, the hand reaming technique used may have variability between tests, and therefore may result in changes to the radio-capitellar and therefore IOM biomechanics.

Among the strengths of this study was the forearm simulator, which allowed a unique perspective on the load transfer characteristics of the forearm. The forearm was tested with minimal constraint while retaining its osseous integrity and an intact soft tissue envelope. Computer controlled dynamic loading enabled accuracy of both axial loads and rotational speeds. A novel approach to IOM tension measurements allowed dynamic and direct measurements of the forces transmitted.

3.5 Conclusion

This study demonstrated that radial head excision markedly increases IOM loading and alters load sharing across the radius and ulna. However, insertion of a correctly sized metallic radial head arthroplasty recreates near normal forearm biomechanics, with no

change in IOM loading characteristics. This information may have a role in clinical decision making as well as the rehabilitation of the forearm after radial head fractures.

3.6 References

[1] Pfaeffle HJ, Fischer KJ, Manson TT, Tomaino MM, Woo SL, Herndon JH: Role of the forearm interosseous ligament: is it more than just longitudinal load transfer? J Hand Surg Am 2000:25;683-688.

[2] Liew VS, Cooper IC, Ferreira LM, Johnson JA, King GJ. The Effect of Metallic Radial Head Arthroplasty on Radiocapitellar Joint Contact Area. Clin Biomech 2003:18(2);115-8.

[3] Charalambous C, Stanley J, Mills S, Hayton M, Hearnden A, Trail I, Gagey O. Comminuted Radial Head Fractures: Aspects of Current Management, Journal of Shoulder and Elbow Surgery, 2011: 996-1007.

[4] Iftimie PP, Garcia JC, Forcada IdLG, Pedrouzo JEG, Goma JG. Resection Arthroplasty for Radial Head Fractures: Long-term Follow-up, Journal of Shoulder and Elbow Surgery, 2011: 20; 45-50.

[5] Schiffern A, Bettwieser SP, Porucznik CA, Crim JR, Tashjian RZ Proximal Radial Drift following Radial Head Resection, Journal of Shoulder and Elbow Surgery , 2011: 20;426-433.

[6] Grewal R, MacDermid J, Faber K, Drosdowech D, King G. Comminuted Radial Head Fractures Treated with a Modular Metallic Radial Head Arthroplasty. Study of Outcomes, Journal of Bone and Joint Surgery, 2006:2192-2200.

[7] Itamura J, Roidis N, Mirzayan R, Vaishnav S, Learch T, Shean C. Radial head fractures: MRI evaluation of Associated Injuries, Journal of Shoulder and Elbow Surgery, 2005:14(4); 421.

[8] Hausmann J, Vekszler G, Mreitenseher M, Braunsteiner T, Vecsei V, Gabler C, Mason Type-I Radial Head Fractures and Interosseous Membrane Lesions - A

Prospective Study, The Journal of Trauma Injury, Infection and Critical Care, 2009:66(2); 457.

[9]   Johnson J, Rath D, Dunning C, Roth S, King G, Simulation of Elbow and Forearm Motion in vitro using a Load Controlled Testing Apparatus, Journal of Biomechanics, 2000:33;635-9.

[10] DeFrate L, Li G, Herndon S, Herndon J, A Minimally Invasive Method for the Determination of Force in the Interosseous Ligament, Clinical Biomechanics, 2001: 895-900.

[11] Markolf K, Lamey D, Yang S, Meals R, Hotchkiss R, Radioulnar Load Sharing in the Forearm: A Study in Cadavera, Journal of Bone and Joint Surgery, 1998: 879-888.

[12] Chadwick E, Nicol A, Elbow and Wrist Joint Contact Forces during Occupational Pick and Place Activities, Journal of Biomechanics, 2000: 591-600.

[13] Shepard M, Markolf K, Dunbar A, Effects of Radial Head Excision and Distal Radial Shortening on Load-Sharing in Cadaver Forearms, The Journal of Bone and Joint Surgery, 2001:93-100.

[14] Manson T, Pfaeffle H,Herndon J, Tomaino M, Fischer K, Forearm Rotation Alters Interosseous Ligament Strain Distribution, Journal of Hand Surgery, 2000: 1058-63.

[15] Rabinowitz R, Light T, Havey R, Gourineni P, Patwardhan P, Sartori M, Vrbos L, The Role of the Interosseous Membrane and Triangular Fibrocartilage Complex in Forearm Stability, Journal of Hand Surgery, 1994: 385-393.

[16] Skahen J, Palmer A, Werner F, Fortino M, The Interosseous Membrane of the Forearm: Anatomy and Function, Journal of Hand Surgery, 1997:22(6); 981-5.

[17] Pfaeffle H, Fischer K, Srinivasa A, Manson T, Woo S, Tomaino M. A Model of Stress and Strain in the Interosseous Ligament of the Forearm Based on Fiber Network Theory, Journal of Biomechanical Engineering, 2006: 725-732.

[18] Gabriel M, Pfaeffle H, Stabile K, Tomaino M, Fischer K, Passive Strain Distribution in the Interosseous Ligament of the forearm: implications for injury reconstruction, Journal of Hand Surgery, 2003: 293-8.

[19] Moritomo H, Noda K, Goto A, Murase T, Yoshikawa H, Sugamoto K, Interosseous Membrane of the Forearm: Length Change of Ligaments During Forearm Rotation, Journal of Hand Surgery, 2009: 685-91.

[20] Rozental T, Beredjiklian P, Bozentka D, Longitudinal Radioulnar Dissociation, Journal of the American Academy of Orthopaedic Surgeons, 2003:11(1);67.

[21] Custers R, Creemers L, van Rijen M, Verbout A, Saris D, Dhert W, Cartilage Damage Caused by Metal Implants Applied for the Treatment of Established Localized Cartilage Defects in a Rabbit Model, Journal of Orthopaedic Research, 2009:84-90.

[22] Popovic N, Lemaire R, Georis P, Gillet P, Midterm Results with a Bipolar Radial Head Prosthesis: Radiographic Evidence of Loosening at the Bone-Cement Interface, The Journal of Bone and Joint Surgery, 2007: 2469-2476.

[23] Morrey B, Radial Head Fracture, in The Elbow and its Disorders, Philadelphia, WB Saunders, 2000:341-363.

[24] Schneiderman G, Meldrum RD, Bloebaum RD, Tarr R, Sarmiento A. The Interosseous Membrane of the Forearm: Structure and Its Role in Galeazzi Fractures, The Journal of Trauma 1993:35(6);879.

[25] Chandler JW, Stabile KJ, Pfaeffle HJ, Li ZM, Woo SLY, Tomaino MM. Anatomic Parameters for Planning of Interosseous Ligament Reconstruction Using Computer Assisted Techniques, The Journal of Hand Surgery 2003:28(1);111.

Chapter 4

The Effect of Radial Head Implant Length on Radiocapitellar Articular Properties and Load Transfer within the Forearm

Overview: *The effect of radial head implant length on forearm biomechanics is not well understood. This study examined the influence of an increase or decrease in radial head implant length on forearm load transfer as measured by interosseous membrane tension, and changes in radiocapitellar contact properties.*

Publication: *Lanting BA, Ferreira LM, Johnson JA, King GJ, Athwal GS. The Effect of Radial Head Implant Length on Radiocapitellar Articular Properties and Load Transfer within the Forearm. J Orthop Trauma. [Epub ahead of print], 2013 Oct*

4.1 Introduction

Radial head fractures are common, with the majority being minimally displaced and successfully treated non-operatively (1). Surgical management may be required for more displaced fractures. Open reduction and internal fixation, while successful for simple displaced fractures, has been less reliable when treating fragmented and osteopenic fractures due to a higher incidence of complications (2). Comminuted radial head fractures have a high incidence of associated ligamentous and osseous injuries, which often precludes radial head excision. For these reasons, radial head arthroplasty is increasingly utilized for fractures with greater levels of comminution with high patient satisfaction (3).

Arthroplasty is technically demanding due to the complex anatomy of the elbow. The combination of osseous comminution and disruption of the soft tissue envelope can make accurate assessment of the appropriate radial head implant length challenging. Although the effect of radial head implant length on forearm biomechanics has not been well delineated, placement of a radial head implant that is longer than the native radial head

has been clinically associated with the development of stiffness, pain and capitellar wear (4,5). The purpose of this study, therefore, was to examine the effect of radial head implant length on forearm biomechanics; specifically the effects of increasing or decreasing implant length on interosseous membrane (IOM) tension and radiocapitellar joint contact area and pressure.

4.2 Materials and Methods

The in-vitro forearm motion simulator described in Chapter 2 was employed. The simulator (Fig. 4.1) was designed to produce axial loading of the forearm while simultaneously generating automated passive pronation and supination. This device allowed unconstrained motion through the carpus, radius, ulna and elbow. The humeral mount permitted medial-lateral translation, varus-valgus angulation, and axial rotation. Multiple degrees of freedom were incorporated into the simulator to ensure adjustability for each specimen, and to allow loading in a physiologic manner with minimal constraint. The metacarpals were potted such that the third metacarpal was in-line with the axis of the applied load (6), and the forearm was aligned with the applied load prior to potting the humerus.
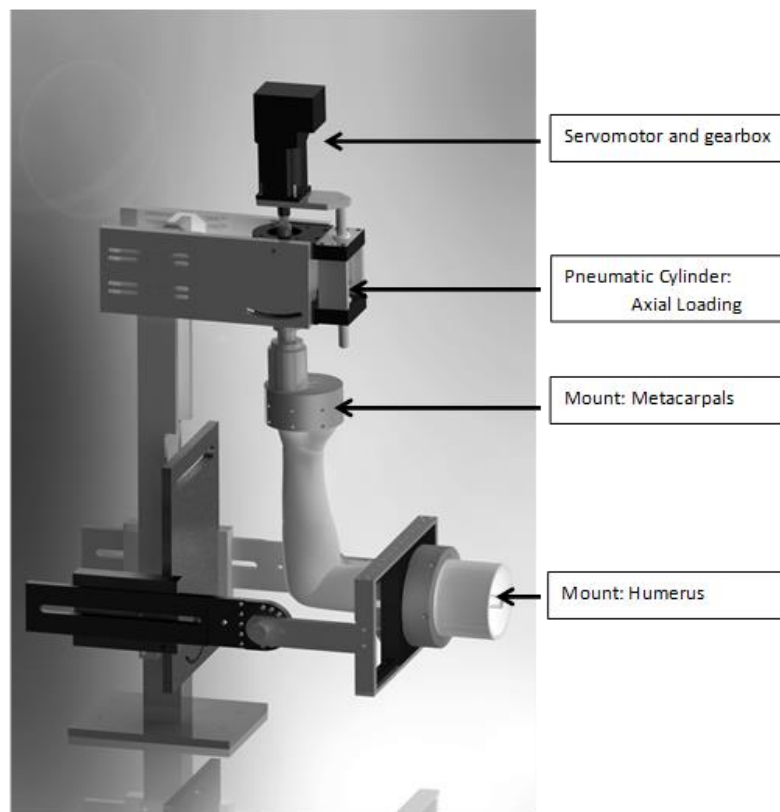
Figure 4.1: The testing simulator, modeled with a specimen mounted in the metacarpal and humeral pots.

Axial loading was applied through the metacarpals by a pneumatic actuator (Model FOD-094-S, Bimba®, University Park, IL) and governed by a custom software controller using closed-loop feedback from a load cell (Futek® Model MBA 600, Irvine, CA). Forearm pronation and supination motion was driven by a servomotor (Model SM2315-DT, Animatics®, Santa Clara, CA), with a cycle of rotation from pronation to supination and back to pronation in six seconds. To measure tension in the interosseous membrane (IOM), a custom load cell was constructed with a pair of strain gauges (Vishay Micro-Measurements®, 120 Ω, 90o rosette, Raleigh, NC) affixed to a strip of spring steel 9.5 x6.5 x 0.32 mm in a layout which compensated for changes in temperature (Fig 4.2). The load cell was designed to be woven over and under the IOM fibers, with its bending axis created via a three point loading construct. The sensor was calibrated by weaving the device through synthetic material and hanging weights on it. Calibrating using excised IOM tissue was not found to be possible due to tissue integrity, calibrating using an IOM with bone blocks not reproducible due to challenges of hanging weights in line with the IOM fibres on obliquely oriented bones. After calibration, the load cell was able to quantify IOM tension in real-time under dynamic loading conditions. Radiocapitellar contact area and pressure were measured in real-time using a flexible, thin pressure sensor array (K-Scan system, Model 4201, I-Scan 5.761 software, Tekscan®, South Boston, MA) interposed in the joint. The position of the inserted Tekscan® was marked. Notably, areas of deformation occurred in the thin flexible transducers at the periphery of the confined space of the radiocapitellar joint. These areas of deformation could not be recreated accurately during calibration attempts between specimens. Therefore, absolute values could not be used, and intra-specimen standardization was conducted to provide a measure of the impact of radial head length without compromising of the integrity of the data presented.

Six cadaveric specimens (mean age 65, range 52-72 yrs) were prepared for testing. The fresh frozen, unembalmed specimens were included only if there was no prior fracture or

Figure 4.2: Load cell sutured to the IOM after being woven into the central band of the IOM

evidence of arthritis, on pre-testing Computed Tomography (CT). The arms were thawed at room temperature for 16 hours. The fingers were disarticulated at the metacarpal-phalangeal joints, and the metacarpals were stripped of all soft tissues. The thumb was disarticulated at the carpo-metacarpal joint. The tendinous insertions to the metacarpal bases were maintained, as were the joint capsules of the wrist and carpal bones. All soft tissue was stripped off the humeral shaft starting 8 cm above the elbow joint. Via a Thompson approach, a dorsal trapdoor was made to access the central band of the IOM, hinging the soft tissue at the ulna. The extensor digitorum communis was resected over the central band of the IOM. The remainder of the musculotendinous units were gently retracted to expose the IOM for a distance of 10 cm directly overlying the central portion of the IOM. The proximal and distal portions of the IOM were sectioned to isolate the central band. Two 8 mm long parallel slits were made 4 mm apart in the central band parallel to the IOM fibers, without damaging the IOM fibres. Both ends of the load sensing device were then inserted into the slits, thus weaving it into the central band of the IOM. Small holes at each end of the load cell were used to secure it to the IOM using 5.0 silk suture (Ethicon, San Antonio, TX).

A steinman pin was placed transversely through the metacarpals and the specimen was positioned with the wrist in neutral in all planes, and potted with the third metacarpal in line with the applied loading vector. After the potting cement had cured, the metacarpal pin was removed. The elbow was flexed to 90°, and the forearm and carpus aligned with the applied axial load. The humerus was potted, and the limits of forearm rotation for each specimen were assessed manually and recorded by servomotor position feedback. These terminal ranges of motion were then precisely repeated by the servomotor throughout all trials. Static muscle forces across the elbow were simulated with weights by suturing cables to the tendons of the brachialis, biceps and triceps tendons using No. 2 Ethibond® (Ethicon, San Antonio, TX). The magnitude of the weights applied were: 2 kg for the brachialis and biceps brachii, and 4 kg for the triceps (7). Muscle lines of action were achieved with an arrangement of adjustable pulleys.

A direct lateral approach to the radial head was performed by splitting the common extensor tendon and the underlying annular ligament. A small portion of the radial collateral ligament was released off the humerus to provide adequate exposure to resect and replace the radial head, but the humeral and ulnar attachments of the lateral ulnar collateral ligament were preserved. A microsagittal saw was used to make the radial neck cut four mm proximal to the head neck junction to allow testing to an increase and decrease of 4 mm in radial head length. The native radial head diameter and length was measured using calipers (Model 500-784, Mitutoyo Digimatic®, +/- 0.01 mm, Mississauga, ON). The native radial head length and diameter were selected to recreate the anatomic size of the native radial head; including the kerf of the saw blade. The native radial head height was defined as 0, or anatomically correct, radial head length. The radial canal was hand reamed and a trial radial stem and head were inserted (Evolve®, Wright Medical Technology, Arlington, TN). The annular ligament, radial collateral ligament and common extensor tendon split were repaired in layers using interrupted No. 2 Ethibond® sutures (Ethicon, San Antonio, TX). The arm was then tested through a full range of pronation and supination for three cycles for each radial head length at 160 N. The axial load applied in this study were higher than in previous reports (8,9,10) to reflect the higher loads that likely occur physiologically (11). IOM tension was measured continuously, with the third cycle used for data analysis. Following testing of each implant size, the sutures were removed, and the pressure sensor was inserted into the radiocapitellar joint. The arm was then tested statically in neutral rotation. The applied load was continuously increased at a rate of 8 N/s to 160 N. Pressure and area measurements were consistently taken three seconds after achieving 160 N of axial load, in order to allow a steady state to be reached. The outcomes were assessed, and consistent areas of deformation were manually removed for both pressure and area measurements. The pressure sensor was then removed, and the next trial radial head implant length was placed. The annular ligament and the common extensor tendon split were repaired between each test condition. The forearm was tested for five radial head implant lengths: -4 mm, -2 mm, 0 mm, +2 mm and +4 mm. The sequence in which the radial head implant lengths were tested was randomized for each specimen.

4.2.1 Statistical Methods

One way and repeated measures ANOVA were utilized to calculate statistical significance, defined as p<0.05, for the dependent variables of IOM tension, contact area and contact pressure. Repeatability was assessed by determining linear dependence using the Pearson correlation coefficient of the IOM load sensor of sequential testing with the same test conditions series. Power analysis was not possible due to the unique nature of testing.

4.3 Results

The simulator was found to provide good repeatability, with the IOM load sensor having a Pearson correlation coefficient of greater than 0.9, and a standard deviation of 0.7%.

Interosseous membrane tension was influenced by radial head length (p=0.006) (Fig 4.3). Average forces recorded in the IOM with a -4 mm radial head length were almost double (310 N +/- 190 N) that of the applied axial load (160N). As radial head implant length increased, IOM tension decreased (p=0.006). When the radial head was lengthened by 4 mm, the IOM was unloaded; recording no load in every specimen. When the radial head was lengthened by 2 mm, the IOM was unloaded in half of the specimens. Only one specimen achieved an IOM tension of greater than 20 N, with a maximum tension of 70 N. IOM tension significantly increased when comparing the optimal radial head length to the -4 mm length implant (p=0.005). IOM tension was not found to significantly increase for the -2 mm radial head length (p=0.288). A negative value of IOM tension is not possible, but the error bars extend to negative values due to the standard deviation of these specimens.

Articular contact area significantly increased with increasing axial loads (p=0.030). Radial head length was not found to have a statistically significant effect on contact area, (p=0.051) (Fig. 4.4). From -4 mm to the correct length, radiocapitellar joint contact area increased with increasing radial head implant length. However, with increased length beyond the correct length (+2 and +4 mm), contact area decreased. Radial head lengths of 2 mm greater or less than that of the correct length did not show any statistically significant difference in contact area in comparison to the correct length.
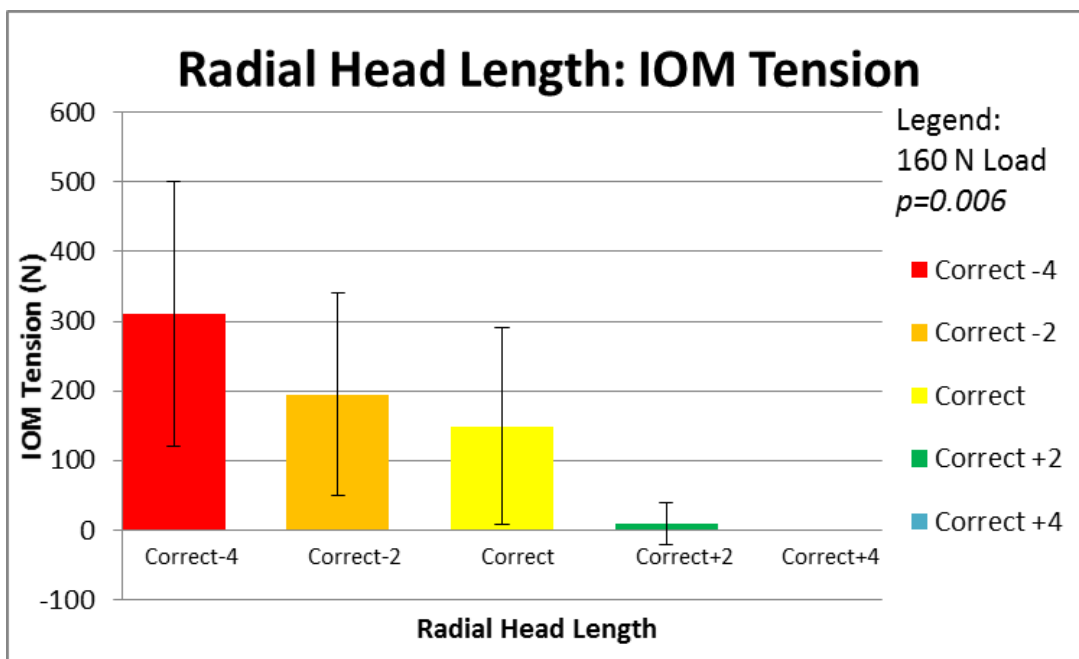
Figure 4.3: The effect of radial head length on IOM tension under 160 N axial loading. Average of six specimens shown with error bars indicating one standard deviation. [IOM: Interosseous membrane]
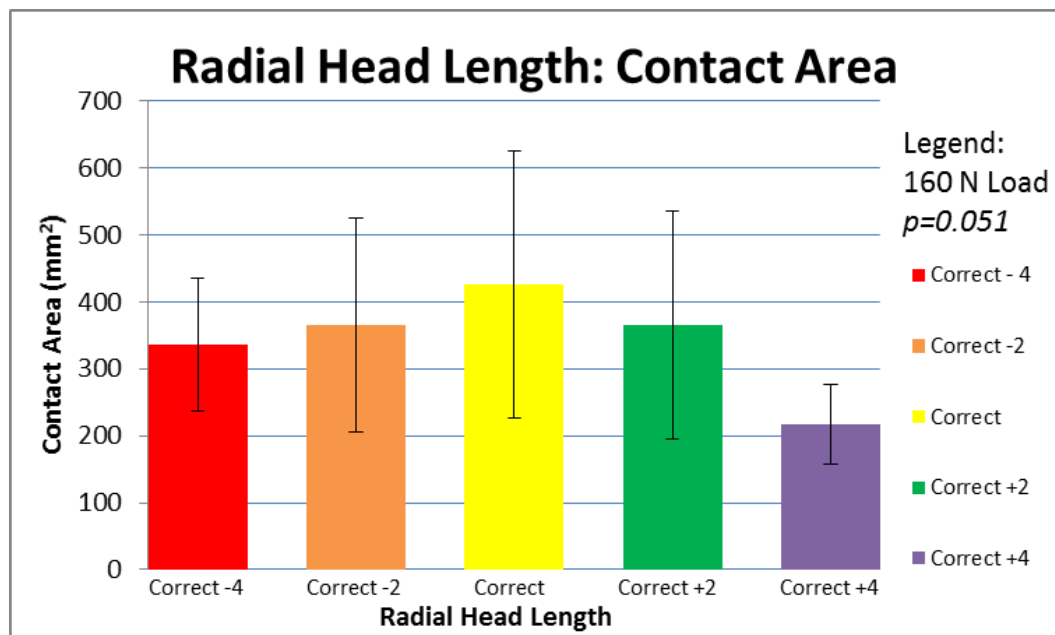
Figure 4.4: The effect of radial head length on radio-capitellar contact area under 160 N of axial load. Demonstrated is an initial increase in contact area as the radial head is lengthened to the anatomically correct length, but then a decrease in contact area as the radial head length is increased beyond this length. Error bars demonstrate one standard deviation

Contact pressures normalized to the anatomically correct length were significantly impacted by changing radial head length (Fig. 4.5) (p=0.021). In pairwise analysis, the contact pressure of the +4mm implants were significantly greater than the – 4mm lengths r (p=0.005). However, a decrease in 2 mm was not found to be statistically different than the correct length in pairwise analysis (p=0.183).

4.4 Discussion

The forearm simulator permitted physiologic testing of the forearm in a repeatable way. This enabled determination of the effect of axial loading and radial head implant length on IOM tension and radiocapitellar contact area and pressure. Direct instrumentation of the IOM with a calibrated strain gauge-based load cell has advantages over calculated IOM tension. In most previous studies, the relationship between the IOM and radio-ulnar loading has been indirectly determined from strain gauges implanted in the osteotomized radius and ulna (12, 6, 13). IOM tension has only been directly measured in one study, using an arthroscopically implantable force probe. However, in this study, osteotomies of the radius and ulna were used, and no radial head arthroplasty group was included (6). Thus, direct comparison to the current study is not possible.

Direct quantification of the IOM loads allowed examination of the influence of radial head implant length on forearm biomechanics and load transfer between the radius and ulna. Increased radial head length effectively unloads the IOM, reducing the loads to near zero. Shortening the radial head implant length by 4 mm produces a significant increase in the IOM tension (p=0.005), while shortening the radial head length by 2 mm does not produce a statistically significant change in IOM tension (p=0.098). This highlights the sensitive nature of load transfer in the forearm to radial head implant length, and the importance of precise recreation of radial head length in order to maintain normal forearm biomechanics. The finding that the IOM loads are higher than the applied axial loads when the radial head length is decreased may to be due to the fact that the fibers of the IOM are oblique to the long axis of the forearm (i.e. the direction of the applied load), thus adding a perpendicular load vector component to the net force in the fibers. Unfortunately, due to the variable angle of insertion on the radius and ulna, calculations could not be made with validity.
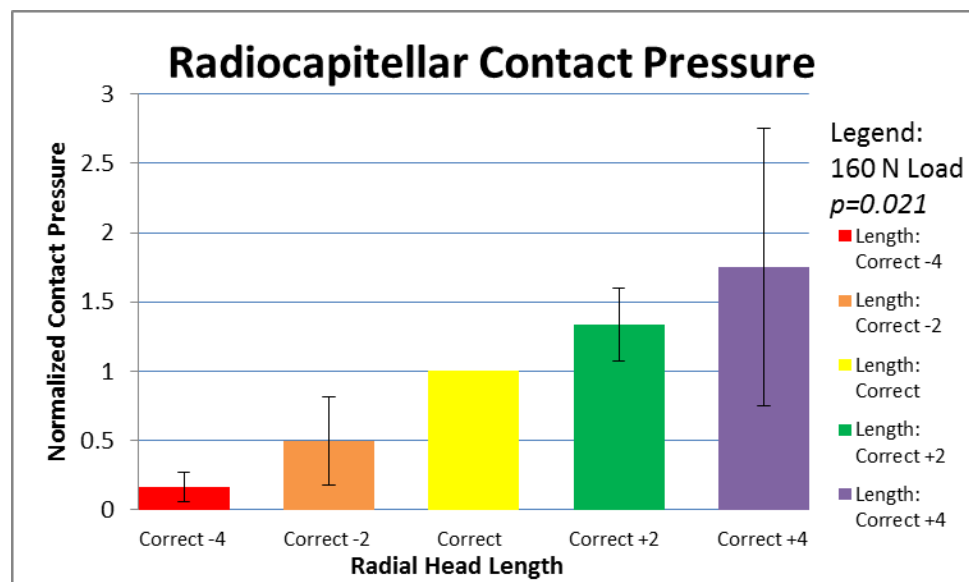
Figure 4.5: The effect of radial head arthroplasty length on contact pressures under 160 N of axial load; where the contact pressures are normalized to the anatomically correct length. Error bars demonstrate one standard deviation.

Radiocapitellar articular contact pressure increased with greater radial head implant length (p=0.021). The finding that contact pressures were not significantly changed when the length of the radial head implant was increased or decreased by 2 mm from optimal may indicate that contact pressure is not as sensitive to radial head implant length as is IOM tension. Alternatively, this could be due to variability in the measurement of contact pressure as a result of transducer positioning or sensitivity. Van Glabbeck et al (2003) published similar findings testing in-vitro with a custom, telescoping radial neck (5). In that study, it was found that an increase in length of the radial head by 2.5 mm increased radiocapitellar pressure through over-stuffing. This is similar to our study findings that indicate increased radial head length increases radiocapitellar pressure, however pairwise comparison of 2 mm increased or decreased from the optimal state did not demonstrate statistical significance.

The measurement of radiocapitellar contact area has previously been reported in a benchtop study albeit at a lower magnitudes of applied load (16). In that study the metallic radial head implants decreased contact area relative to the native articulation, potentially due to the implant geometry. However, the effect of radial head implant length on contact area has not been previously reported within an intact forearm. Contact area results differed from expected values. Notably, contact area decreased if the radial head length increased or decreased, resulting in no statistically significant relationship of radial head length to contact area. Intuitively, increased radiocapitellar force should increase contact area as the capitellar cartilage and bone deforms (17). Given that increased radial head length unloads the IOM, resulting in increased loads at the viscoelastic radiocapitellar joint, it was expected that the contact area would correspondingly increase with increased radial head implant length. However, this was only observed when radial head length was increased up to the anatomically correct length. Radiocapitellar contact area diminished with increased radial head length in spite of increased radiocapitellar average pressure. Future studies should track the kinematics of the implant with respect to the capitellum to evaluate this finding. Other literature indicates that a change in radial head length impacts the motion kinematics of the forearm, which may also impact the radiocapitellar alignment (5). Also, the soft tissues of the direct lateral approach could not be repaired for this portion of testing to allow

egress of the pressure sensor wires. This alteration of the soft tissue envelope could impact the radiocapitellar articular alignment by causing non-distributed point loading.

The findings of this study are concerning for the health of capitellar cartilage in the setting of an over-lengthened radial head implant. With radial head replacement, the radiocapitellar surface is comprised of metal articulating on cartilage, which has been shown to be detrimental to cartilage in animal models (18). Our data demonstrates that increased radial head implant length beyond the anatomically correct length unloads the IOM. It is known that 80% of loads applied to the carpus are transferred to the distal radius, but only 40-60% of the applied load is transmitted by the radiocapitellar joint (8). The IOM has an important role in that load transfer. It has also been shown that the contact area decreases with radial head implant lengths greater than optimal. Increased radiocapitellar loads and decreased contact areas would be predicted to result in increased contact pressures, which was also quantified in the current study and was confirmed to increase as expected. In addition to the non-physiologic loading of metal on cartilage, increased cartilage wear of the capitellar surface can therefore be expected unless radial head implant length is carefully recreated. Reports describing capitellar erosions and cartilage thinning after radial head implantation confirm the clinical impact of these in-vitro findings (19).

Although an increase in radial head length is clearly detrimental to physiologic load transfer in the forearm and to radiocapitellar articular characteristics, shortening the radial head by 2 mm did not have the same impact. Of particular interest is that shortening the radial head by two mm did not have a statistically significant impact on IOM tension (p=0.29), radiocapitellar contact area (p=0.20), or radiocapitellar articular pressures(p=0.18). However, lengthening the radial head by 2 or 4 mm as well as decreasing the length by 4 mm were shown to have a statistically significant impact on IOM tension and radiocapitellar contact pressure. It is interesting that changes in length did not effect contact area, whereas increased applied load did. This may be due to changes in alignment at the radiocapitellar joint due to length. Decision making intra-operatively can be challenging due to radial head comminution, anatomic anomalies, or when the measured length falls between implant sizes. If the decision between radial

head prosthesis lengths is not clear intra-operatively, the selection of the radial head that is slightly shorter may, in light of the current findings, be advisable to optimize forearm load transfer and radiocapitellar articulation characteristics and represent a clinical safe-zone.

This was an in-vitro cadaveric study using static loading with donor specimens, which has inherent limitations. Whether the results can be applied to younger patients in-vivo remains to be confirmed. Although isolation of the central band of the IOM and potential for deformity on insertion may be a weakness, it was done in recognition of the fact that the central band is the most important portion of the IOM (13), and that it is a discrete structure amenable to the novel measurement techniques used. Finally, absolute values for the pressure sensor could not be used, limiting the ability to correlate these findings to known properties of articular cartilage.

Among the strengths of this study was the sophisticated forearm simulator, which allowed a unique perspective on the load transfer characteristics of the forearm. The forearm was tested with minimal constraint while retaining its osseous integrity and an intact soft tissue envelope. Computer controlled dynamic loading enabled accuracy of both axial loads and rotational speeds. A novel approach to IOM tension measurements allowed dynamic and direct measurements of the forces transmitted. Measurement of the contact area and pressure allowed the load transfer from the radius to the ulna via the IOM and radiocapitellar articular properties to be further characterized. Examination of these outcomes while testing different radial head implant lengths allowed information regarding the effect of over- and under-lengthening to improve our understanding of the importance of radial head implant length.

4.5 Conclusion

Increasing the radial head implant length beyond the correct length was found to increase the radiocapitellar joint contact pressure, decrease joint contact area, and decrease IOM loads. Therefore, restoration of anatomic radial head length is critical when performing radial head arthroplasty in order to maintain normal forearm biomechanics. If the native radial head length is difficult to accurately assess, due to comminution etc, avoidance of

increasing the length of the radial head is important to prevent detrimental changes in the biomechanics of the forearm and the potential for clinically important radiocapitellar joint pathology.

4.6 References

1. Morrey, BF. Radial Head Fracture. The Elbow and its Disorders. Philadelphia : WB Saunders, 2000, pp. 341-363.

2. Charalambos PC, Stanley JK, Mills SP, et al. Comminuted Radial Head Fractures: Aspects of Current Management. Journal of Shoulder and Elbow Surgery. 2011;20:996-1007.

3. Grewal R, MacDermid JC, Faber KJ, et al. Comminuted Radial Head Fractures Treated with a Modular Metallic Radial Head Arthroplasty. Study of Outcomes. J of Bone and Joint Surg. 2006;88(10):2192-2200.

4. Frank SG, Grewal R, Johnson JA, et al. Determination of Correct Implant Size in Radial Head Arthroplasty to Avoid Overlengthening. J of Bone and Joint Surg. 2009;91(7):1738-1742.

5. Van Glabbeek F, Van Riet RP, Baumfeld JA, et al. Detrimental Effects of Overstuffing or Understuffing with a Radial Head Replacement in the Medial Collateral Ligament Deficient Elbow. J of Bone and Joint Surg. 2004;86-A(12):2629-2635.

6. Shepard M, Markolf K, Dunbar A. Effects of Radial Head Excision and Distal Radial Shortening on Load-Sharing in Cadaver Forearms. J of Bone and Joint Surg. 2001;83-A(1):93-100.

7. Johnson JA, Rath DA, Dunning CE, et al. Simulation of Elbow and Forearm Motion in vitro using a Load Controlled Testing Apparatus. J of Biomech. 2000;33:635-639.

8. Pfaeffle HJ, Fischer KJ, Manson TT, et al. Role of the Forearm Interosseous Ligament: Is it more than just Longitudinal Load Transfer. J of Hand Surg. 2000;25(4):683-688.

9. DeFrate LE, Li G, Zayontz SJ, et al. A Minimally Invasive Method for the Determination of Force in the Interosseous Ligament. Clin Biomech. 2001;16(10):895-900.

10. Markolf KL, Lamey D, Yang S, et al. Radioulnar Load Sharing in the Forearm: A Study in Cadavera. J of Bone and Joint Surg. 1998;80(6):879-888.

11. Chadwick, E and Nicol, A. Elbow and Wrist Joint Contact Forces during Occupational Pick and Place Activities. J of Biomech. 2000;33(5):591-600.

12. Manson TT, Pfaeffle HJ, Herndon JH, et al. Forearm Rotation Alters Interosseous Ligament Strain Distribution. J of Hand Surg. 2000;25(6):1058-1063.

13. Rabinowitz RS, Light TR, Havey RM, et al. The Role of the Interosseous Membrane and Triangular Fibrocartilage Complex in Forearm Stability. J of Hand Surg. 1994;19(5):385-393.

14. Gabriel MT, Stabile KJ, Tomaino MM, et al. Passive Strain Distribution in the Interosseous Ligament of the forearm: implications for injury reconstruction. J of Hand Surg. 2003;29(2): 293-298.

15. Moritoma H, Noda K, Goto A, et al. Interosseous Membrane of the Forearm: Length Change of Ligaments During Forearm Rotation. J of Hand Surg. 2009;34(4):685-691.

16. Liew VS, Cooper K, Ferreira LM, et al. The Effect of Metallic Radial Head Arthroplasty on Radiocapitellar Joint Contact Area. Clin Biomech. 2003;18(2):115-118.

17. Spahn, G and Wittiq, R. Biomechanical properties of Hyaline Cartilage under Axial Load. 2003, Zentralbl Chir. 2003;128(1):78-82.

18. Custers RJH, Creemers LB, Van Rijan MHP, et al. Cartilage Damage Caused by Metal Implants Applied for the Treatment of Established Localized Cartilage Defects in a Rabbit Model. J of Orthop Res. 2009;27(1):84-90.

19. Popovic N, Lemaire R, Georis P, et al. Midterm Results with a Bipolar Radial Head Prosthesis: Radiographic Evidence of Loosening at the Bone-Cement Interface. J of Bone and Joint Surg. 2007;89(11):2469-2476.

Chapter 5

Radial Head Implant Diameter: A Biomechanical Assessment of the Forgotten Dimension

Overview: *Current research in how radial head arthroplasty changes the biomechanics*

of the forearm is concentrated on radial head length. However, the radial head diameter

also varies, and the changes in the biomechanics of the forearm secondary to radial head

diameter is unknown. This study examined the influence of radial head implant diameter

on forearm load transfer as measured by interosseous membrane tension and

radiocapitellar joint contact characteristics.

Publication: *Revisions of manuscript requested by Clinical Biomechanics*

5.1 Introduction

Radial head arthroplasty for comminuted radial head fractures results in high patient

satisfaction, and therefore has become increasingly utilized.(1) However, comminuted

radial head fractures have a high incidence of associated soft tissue injuries, of which the

interosseous membrane (IOM) is of notable concern.(2) A number of studies have

emerged about the importance of establishing the correct length of a radial head

implant.(3-5) The concept of insertion of a radial head implant that is too thick has been

termed 'over-lengthening'.(3) It has been demonstrated that increasing the length of the

radial head changes the biomechanics of the forearm, with primary impact at the

radiocapitellar joint.(3) This has led to the understanding that the relationship between

the radius and the ulna is complex and the forearm itself can be considered a complex

articulation.(6) Little consideration, however, has been given to understanding the

impact of changes of the radial head diameter on forearm biomechanics. The influence

of diameter on the magnitude and position of IOM tension is unknown. Moreover, how the radial head diameter impacts the radiocapitellar joint contact area and forces is also unknown. Therefore, the purpose of this study was to examine the impact of radial head implant diameter on radiocapitellar contact area and force as well as the tension within the IOM.

5.2 Materials and Methods

The simulator described in Chapter 2 was used for this study. Loading and motion of the forearm was conducted under computerized control via closed-loop feedback from a load cell (Futek® Model MBA 600, Irvine, CA) as well as position control. Axial loading was applied in line with the third metacarpal using a pneumatic actuator (Model FOD-094-S, Bimba®, University Park, IL). The forearm was rotated through a full range of supination and pronation in six seconds by using a servomotor (Model SM2315-DT, Animatics®, Santa Clara, CA). The ability to constrain specific degrees of freedom allowed focused testing. The simulator also allowed the testing through a range of axial loads both dynamically as well as statically.

The IOM tension was measured using a custom load cell. This load cell was made by applying a pair of strain gauges (Vishay Micro-Measurements®, 120 Ω, 90º rosette, Raleigh, NC) to a strip of spring steel 9.5 x6.5 x 0.32 mm. Based on a three point bending principle, the strain gauge was woven into the central band of the IOM. The load cell was placed through two small parallel cuts made 4 mm apart in line with the fibers of the central band of the IOM, and affixed there by 5.0 silk suture (Ethicon, San Antonio, TX).

The radiocapitellar joint properties were measured utilizing flexible, thin pressure sensor array (K-Scan system, Model 4201, I-Scan 5.761 software, Tekscan®, South Boston, MA). The radiocapitellar contact area and force were measured in situ. The space available for the sensor was limited; resulting in some deformity of the sensor when in place. It was found in trial specimens that the calibration outside of the arm was not possible due to an inability to accurately recreate the areas of deformity, and therefore the data was normalized to the optimal radial head implant diameter and then statistically analyzed.

Five male cadaveric specimens (mean age 65, range 52-72 yrs) were thawed at room temperature. Specimens were excluded if there was Computed Tomography (CT) evidence of a prior fracture or evidence of arthritis. The central band of the IOM was approached via a trap-door skin incision that hinged on the radius. The extensor digitorum communis was excised over the central band, and the load cell was woven into the IOM after retracting the remainder of the muscles. While the central band was retained, the remainder of the IOM was released off the radius and the ulna. The soft tissues were stripped off the metacarpals and the digits were disarticulated at the metacarpophalangeal joints. The soft tissues were also stripped off the humerus; starting 8 cm above the elbow joint. The humerus and metacarpals were potted in polymethylmethacrylate, taking great care to line up the third metacarpal with the applied axial load. Each specimen was tested within the range of motion determined for the individual specimen.

A common extensor tendon split approach was utilized to access the radiocapitellar joint and radial head. The annular ligament was divided and the radial head exposed. The

lateral ulnar collateral ligament was preserved; however, a portion of the radial collateral ligament was elevated off the humerus to obtain sufficient exposure of the radial head. After cutting the radius at the radial neck using a microsagittal saw, the radial head was measured using digital calipers (Model 500-784, Mitutoyo Digimatic®, +/- 0.01 mm, Mississauga, ON). The radial head arthroplasty was sized to match the outer minor articular diameter of the native radial head, and this was defined as the anatomically correct head size. After hand reaming the canal, a metal CoCr monopolar radial head trial (Evolve ®, Wright Medical, Arlington, Tennessee, USA) was inserted, with the smooth stem being implanted in the radial canal. No. 2 Ethibond® suture (Ethicon, San Antonio, TX) was used to repair the common extensor tendon and the annular ligament in layers.

Two testing protocols were utilized. In both, 160 N axial loads were applied to reflect physiologic loads that are thought to occur clinically.(7) The dynamic loading algorithm applied a constant axial load to the forearm with the elbow flexed to 90° through a full range of pronation and supination motion. A complete forearm rotational cycle was programmed to take 6 seconds. The third recorded cycle was utilized for continuous IOM tension data collection. The static loading algorithm also positioned the elbow at 90°, and in neutral forearm rotation. The load was increased at a constant rate of 8 N/s, and the IOM tension was continuously measured. The radiocapitellar joint contact area and pressure were measured three seconds after 160 N had been applied to allow a steady state to be achieved. The order in which radial head sizes (-2 mm, 0 mm and +2 mm) were tested were randomized.

5.2.1 Statistical Methods:

Repeated measures ANOVA was utilized to calculate statistical significance, defined as $p<0.05$, for the dependent variables of IOM tension, contact area and contact pressure.

5.3 Results

The simulator was found to provide good repeatability, with the IOM load sensor having a Pearson correlation coefficient of greater than 0.9, and a standard deviation of 0.7%.

The radiocapitellar contact mechanics were not affected by a change in radial head arthroplasty diameter. At 160 N of axial load, the contact area was not found to differ if the radial head was increased or decreased in diameter by 2 mm (Fig. 5.1) ($p=0.5$). Additionally, contact forces were not impacted by changes in radial head diameter (Fig. 5.2) ($p=0.4$).

The IOM tension was found to be sensitive to radial head diameter ($p=0.01$). Increasing the head diameter increased IOM tension (Fig. 5.3). Increasing the radial head diameter from -2 to +2 increased the IOM tension 36% relative to the -2 mm head diameter.
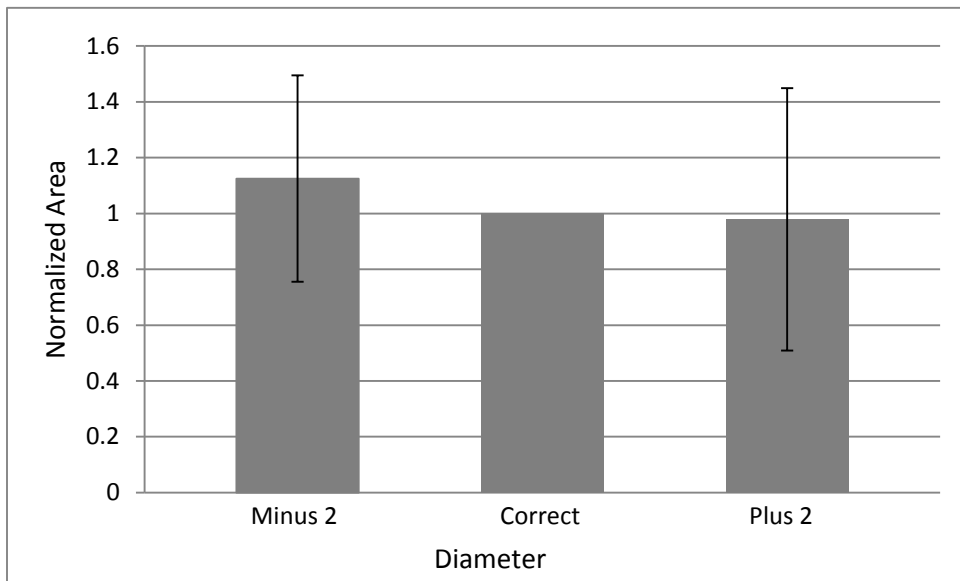
Figure 5.1 The effect of radial head diameter on radiocapitellar contact area when tested in neutral; normalized to the correct radial head diameter (p=0.5)
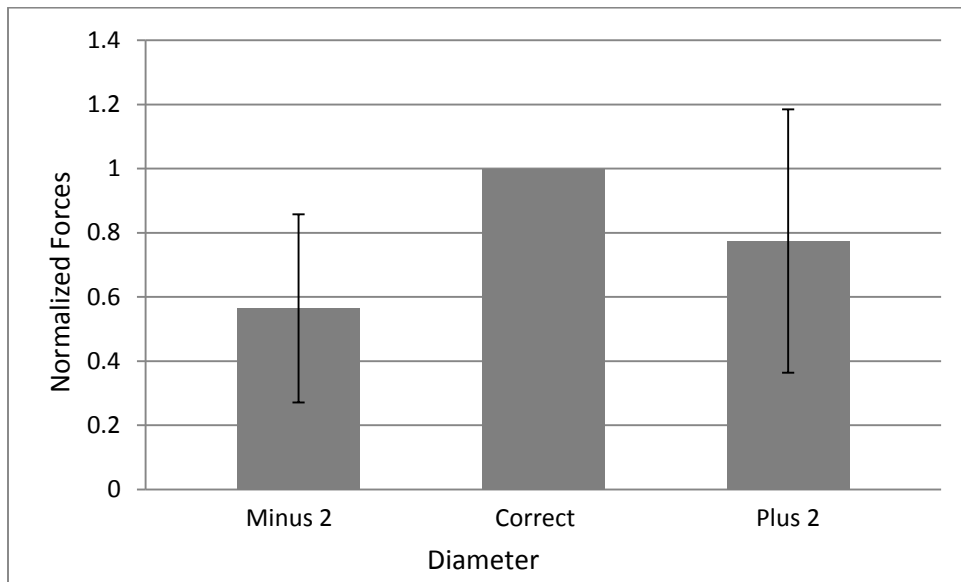
Figure 5.2 The impact of radial head diameter on radiocapitellar contact forces when tested in neutral; normalized to the correct radial head diameter (p=0.4)
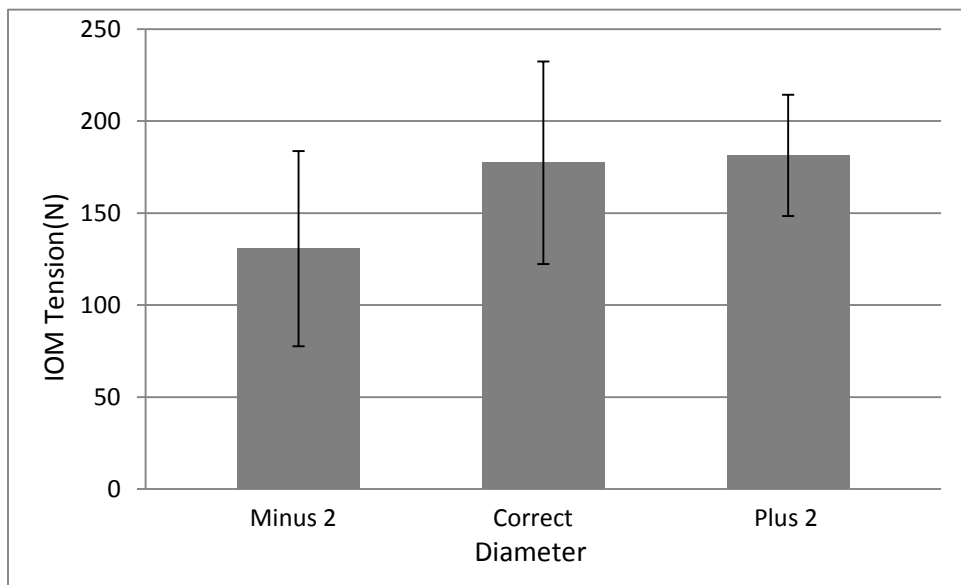
Figure 5.3 The impact of changes in Radial Head Diameter on IOM Tension when tested through pronation and supination (p=0.01)

5.4 Discussion

Direct quantification of the IOM loads allowed examination of the influence of radial head implant diameter on forearm biomechanics and load transfer between the radius and ulna. Radial head implant diameter was found to have a significant impact on IOM tension ($p=0.01$). Increasing the radial head diameter increased IOM tension. An increase in diameter by four mm increased IOM tension by 36% relative to the -2 mm diameter. This increase in IOM tension will have an impact on proximal radioulnar joint (PRUJ) forces. The increase in forces between the radius and ulna may compromise the radial head arthroplasty, with potential for stem loosening or the development of cartilage erosions within the lesser sigmoid notch; both of which may lead to pain.

Radiocapitellar contact area was not impacted by changes in radial head diameter within the range of implant diameters tested. Although the absolute values decreased with increased diameter, this was not statistically significant ($p=0.5$). A decrease in contact area with increased diameter is consistent with other literature.(8) Liew et al found that decreased radial head diameter increased contact area, and it was suggested that this was due to an increased conformity of the radial head arthroplasty. Additionally, contact forces were not affected by changes in radial head diameter within the range of implant diameters tested. Although the absolute value of the contact forces appeared to show a decrease in contact area if the diameter was increased or decreased, this was not statistically significant ($p=0.4$).

The forearm simulator permitted physiologic testing of the forearm in a repeatable way. This enabled determination of the effect of radial head implant diameter on IOM tension and radiocapitellar contact area and pressure. Direct instrumentation of the IOM with a

calibrated strain gauge-based load cell has advantages over calculated IOM tension. In previous studies, the relationship between the IOM and radio-ulnar loading has been indirectly determined from strain gauges implanted in the osteotomized radius and ulna.(9-11) Direct instrumentation preserves the osseous integrity, and therefore measured values are more likely to represent actual values.

The radial head replacement used has a symmetric geometry, and differs from the elliptoid shape of the native radial head. It is not a cemented stem, and motion between the stem and the radius can occur. This differs from other designs on the market. The use of a cemented, rigidly fixed stem or a prosthesis that more closely replicates the native radial head may change the outcomes found.

This was an *in-vitro* cadaveric study with a small number of donor specimens, which has inherent limitations. TekScan sensor limitations prevented the use of absolute values. Isolation of the CB of the IOM was done as the CB is the most important portion of the IOM. However, measurement of only the CB may be considered a weakness. Measurement of the forces through the central band of the IOM only without instrumentation of other portions of the membrane may be a weakness; but the central band is known to be the most important portion of the IOM.(11) As measurement of the forces at the PRUJ was not done, thoughts on overstuffing the PRUJ via increases in radial head diameter are a hypothesis only.

This study had a number of strengths. The simulator allowed computer controlled testing with minimal constraint and an intact boney structure under dynamic and static loading conditions. With the majority of the soft tissue environment intact, measurements of the

load transfer within the forearm were possible in a non-invasive and continuous manner.

The measurement of contact area and contact force allowed correlation to the IOM

tension. Examination of these outcomes while testing different radial head implant

diameters allowed a unique perspective of the impact of radial head diameter changes; an

area that is not well understood.

5.5 Conclusions

Changes to radial head implant diameter does not significantly change radiocapitellar

contact area or contact forces. However, increasing the radial head diameter was found

to significantly increase IOM tension.

5.6 References

1. Grewal R, MacDermid J, Faber K, Drosdowech D, King G. Comminuted Radial Head Fractures Treated with a Modular Metallic Radial Head Arthroplasty. Study of Outcomes, Journal of Bone and Joint Surgery, 2006:2192-2200.

2. Hausmann JT, Vekszler G, Breitenseher M, Braunsteiner T, Vecsei V, Gabler C. Mason Type-I Radial Head Fractures and Interosseous Membrane Lesions - A Prospective Study. The Journal of Trauma Injury, Infection and Critical Care, 2009:66;457.

3. Van Glabbeek F, Van Riet RP, Baumfeld JA, Neale PG, O'Driscoll SW, Morrey BF, An KN. Detrimental Effects of Overstuffing or Understuffing with a Radial Head Replacement in the Medial Collateral Ligament Deficient Elbow. The Journal of Bone and Joint Surgery, 2004:86-A(12) 2629-2635.

4. Doornberg JN, Durk SL, Zurakowski D. Reference Points for Radial Head Prosthesis Size. Journal of Hand Surgery, 2006:31A; 53-7.

5. Frank SG, Grewal R, Johnson J, Faber KJ, King GJ, Athwal GS. Determination of Correct Implant Size in Radial Head Arthroplasty to Avoid Overlengthening. The Journal of Bone and Joint Surgery, 2009:91(7); 1738-1742.

6. Tang P, Failla JM, Contesti LA. The Radioulnar Joints and Forearm Axis: Surgeon's Perspective. Journal of Hand Therapy, 1999:12(2); 75-84.

7. Chadwick, E and Nicol, A. Elbow and Wrist Joint Contact Forces during Occupational Pick and Place Activities. Journal of Biomechanics, 2000:33(5);591-600.

8. Liew VS, Cooper IC, Ferreira LM, Johnson JA, King GJ. The Effect of Metallic Radial Head Arthroplasty on Radiocapitellar Joint Contact Area. Clin Biomech 2003:18(2);115-8.

9. Shepard, M, Markolf, K and Dunbar, A. Effects of Radial Head Excision and Distal Radial Shortening on Load-Sharing in Cadaver Forearms. The Journal of Bone and Joint Surgery, 2001:83-A(1);93-100.

10. Manson TT, Pfaeffle HJ, Herdon JH, Tomaino MM, Fischer KJ. Forearm Rotation Alters Interosseous Ligament Strain Distribution. Journal of Hand Surgery, 2000:25(6):1058-1063.

11. RS Rabinowitz, TR Light, RM Havey, P Gourineni, AG Patwardhan, MJ Sartori, L Vrbos. The Role of the Interosseous Membrane and Trigangular Fibrocartilage Complex in Forearm Stability. The Journal of Hand Surgery, 1994:19(3);385-393.

Chapter 6

Conclusions and Future Directions

6.1 Conclusions: Clinical Relevance

As part of this treatise, a forearm simulator was designed, built and validated to allow testing in a way that more closely paralleled a physiologic environment. This simulator allowed testing of multiple clinically relevant biomechanical scenarios of the forearm, while retaining as much of the soft tissue envelope as possible. Testing was possible in multiple positions of elbow flexion and extension under controlled axial loads and simulated passive forearm rotation. Unique measurement tools were utilized to quantify the biomechanics of targeted structures in the forearm.

The clinical area that was focused on for this study was fractures of the radial head, which are common. While reconstruction of the radial head is the preferred treatment for displaced fractures, comminution may prevent the successful repair of the radial head. These patients are usually treated with radial head excision or arthroplasty. It is also known that in long term studies, patients treated with a radial head excision have an increase in valgus angulation and have proximal radial migration.(1) Our data demonstrated that radial head excision results in significant changes to forearm biomechanics; with a marked increase in interosseous membrane (IOM) loading. Understanding the increased IOM tension that occurs secondary to radial head excision may provide an explanation for the proximal migration. The importance of this finding may be increased by understanding that IOM injuries have been known to occur in up to 2/3rds of all patients in whom a Mason I radial head fracture has occurred.(2) The increased IOM tension has implications on rehabilitation as well. The good clinical outcomes of radial head arthroplasty has been published.(3) It is notable that the patients have largely recovered within six months, with minimal recovery after that. This has lead to review papers suggesting that in some patients, radial head replacements are the preferred treatment.(1)

A correctly sized metallic radial head arthroplasty recreates near normal forearm biomechanics. However, increasing the radial head implant length beyond normal was found to increase the radiocapitellar joint contact pressure, decrease joint contact area, and decrease IOM loads. Changes in radial head implant diameter did not significantly change radiocapitellar contact area or contact forces but increasing the radial head diameter was found to significantly increase IOM tension. This may have significant clinical relevance. Increased IOM tension may result in mid forearm pain or increased PRUJ force and subsequent pain at the elbow. Increased PRUJ forces may result in increased forces at the radial head replacement stem. Literature has been published on the periprosthetic radiolucency at the radial head stem in over half of the patients assessed.(4) Further study to examine the clinical and biomechanical effect of radial head diameter is warranted.

Collectively these studies suggest that a careful measurement of the excised bone fragments is important to ensure that a radial head arthroplasty restores the size of the native radial head. Anatomic radial head length is critical when performing radial head arthroplasty in order to maintain normal forearm biomechanics and load transfer. Over-lengthening of the native radial head should be avoided to prevent detrimental changes in the biomechanics of the forearm with overloading of the capitellar cartilage and the development of secondary degenerative changes. Radial head implant diameter is also important to consider as increasing the radial head diameter increases IOM tension which may lead to the development of forearm pain or cartilage overloading of the radial notch of the ulna and arthritis of that articulation. Our data supports the beneficial biomechanical effects of radial head replacement rather than excision, and the need for more accurate techniques to optimize implant sizing.

6.2 Future Directions

The forearm simulator will allow improvements in our understanding of forearm biomechanics in other clinically relevant scenarios such as bony and soft tissue disorders of the wrist, distal radioulnar joint, midshaft and elbow. The measurement technique to assess IOM tension was unique, and can also be employed in future studies. Changes in

the rate of axial loads and forearm rotation will allow further understanding of the biomechanics of the forearm. The biomechanical information gained in this study may allow computational modelling of forearm biomechanics. Finally, the passive motion and loading model used could be changed to active motion and loading to incorporate the dynamic units of the forearm.

Our data provides a better understanding of how changes to the radial head effect forearm biomechanics. This information can be used as a basis for clinical trials and focused clinical questions. The improved understanding of the biomechanics of the forearm can also be used to optimize rehabilitation protocols.

6.3 References

1. Charalambous C, Stanley J, Mills S, Hayton M, Hearnden A, Trail I, Gagey O. Comminuted Radial Head Fractures: Aspects of Current Management, Journal of Shoulder and Elbow Surgery, 2011: 996-1007.

2. Hausmann JT, Vekszler G, Breitenseher M, Braunsteiner T, Vecsei V, Gabler C: Mason type-I radial head fractures and interosseous membrane lesions--a prospective study. J Trauma 66:457-461, 2009

3. Grewal R, MacDermid J, Faber K, Drosdowech D, King G. Comminuted Radial Head Fractures Treated with a Modular Metallic Radial Head Arthroplasty. Study of Outcomes, Journal of Bone and Joint Surgery, 2006:2192-2200.

4. Popovic N, Lemaire R, Georis P, Gillet P, Midterm Results with a Bipolar Radial Head Prosthesis: Radiographic Evidence of Loosening at the Bone-Cement Interface, The Journal of Bone and Joint Surgery, 2007: 2469-2476.

Appendix 1:

Design Images of the Forearm Simulator
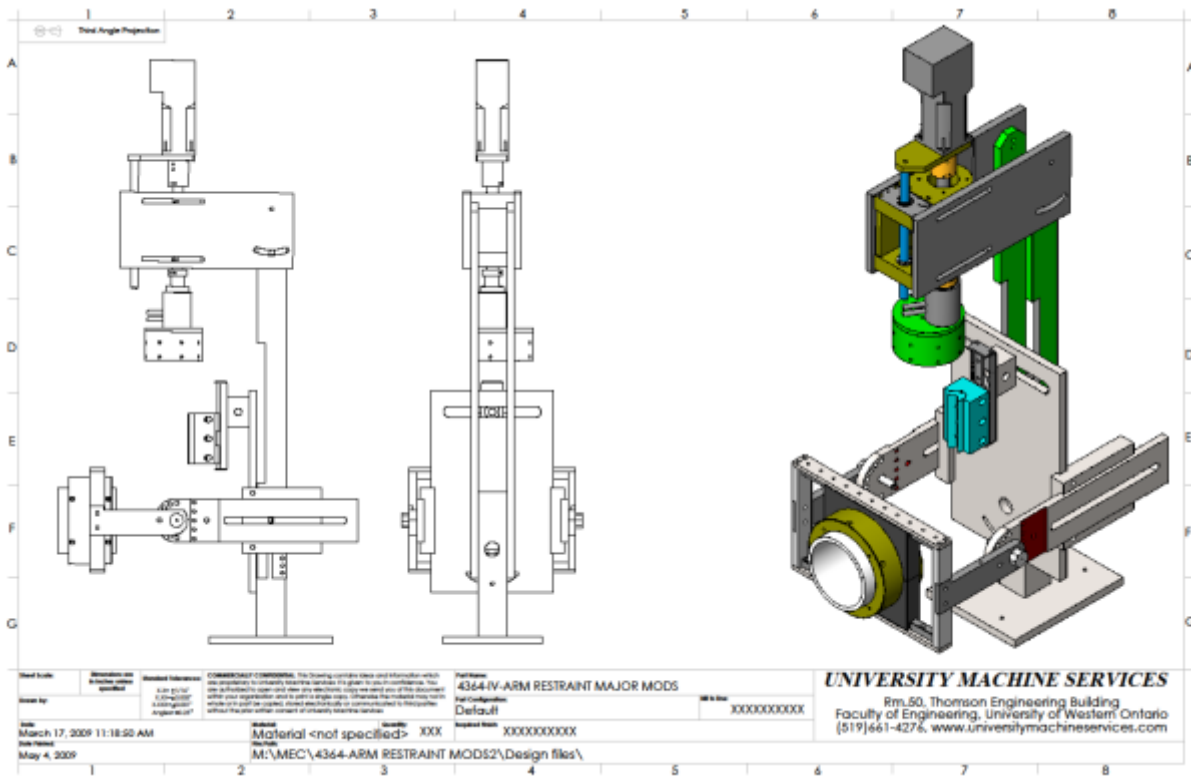
Appendix 1: Forearm Simulator, shown with orthogonal and isometric views

Appendix 2:

The Servomotor

Appendix 2: The servomotor and gearbox, utilized to create the appropriate torque

Appendix 3:

The Pneumatic Cylinder
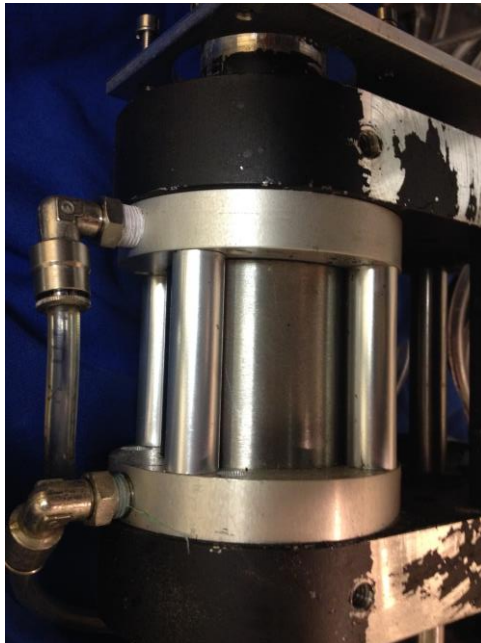
Appendix 3: The double acting, double ended pneumatic cylinder utilized

Appendix 4:

The Load Cell

Appendix 4: Load Cell; capable of measuring axial loads as well as torque

Appendix 5:

The Articular Sensor
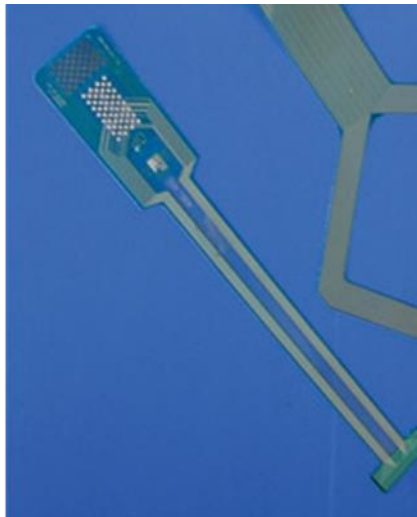
Appendix 5: Contact pressure and area sensor (TekScan ®) that was utilized

Appendix 6:

Optic Trackers

(A)

(B)
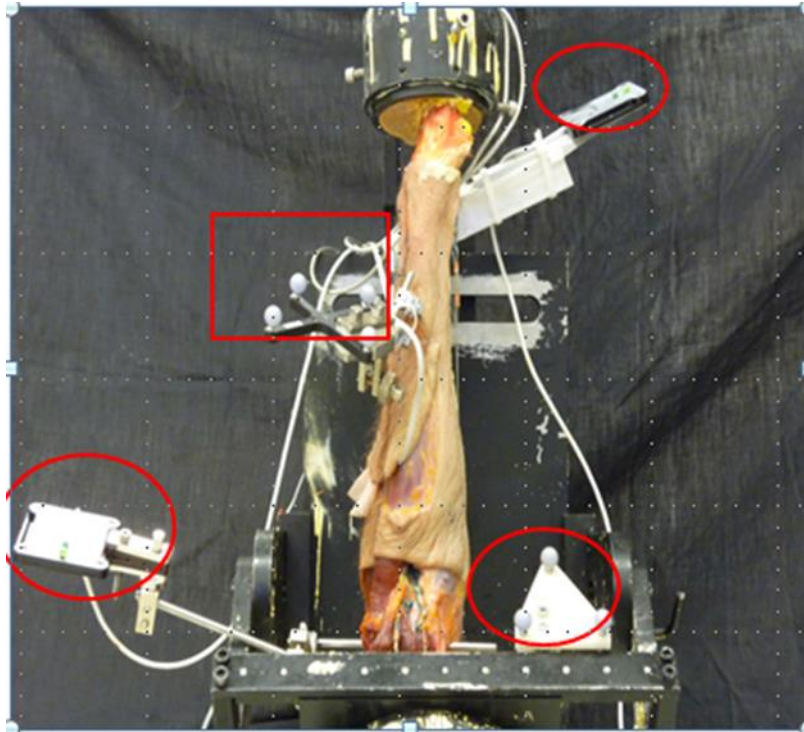
Appendix 6: The simulator was designed to also facilitate optic tracking of the rigid bodies of the forearm as required. Testing with both passive trackers (A) and active (circled, B) was conducted.

Appendix 7: Glossary

ADL   - Activities of daily living

Anatomic   - Relating to the structure of the body

Anterior   - Towards the front of the body

Annular Ligament   - A ligament which encircles the head of the radius ensuring
                               contact between the radius and PRUJ

Arthroplasty   - Surgical reconstruction or replacement of a joint

Articular   - Relating to a joint

AB   - Accessory band
Capitellum   - Smooth rounded surface on the lateral distal humerus
                               which articulates with the radial dish

Cartilage   - Smooth, firm connective tissue found on articulating surfaces of
                               joints

CB   - Central band

Circumduction   - Describes the motion of a long bone when its distal end
                               circumscribes the base of a cone

Comminuted   - To break into several small fragments

Contact Area   - Surface area in contact between two bones

Coronal   - A vertical plane which divides the body into anterior and
                               posterior portions

Coronoid   - Triangular anterior projection on the proximal ulna which
                               articulates with the radius

Distal   - Away from the center of the body

DOC   - Distal oblique cord

DRUJ   - Distal radioulnar joint, pivot-joint between the distal radius and

                          ulna

Epicondyle   - A projection close to a knuckle shaped surface (ie: condyle),

                          usually serving as a point of attachment for ligaments from an

                          adjacent joint or muscle group

Excision   - Surgical removal

Extension   - The act of straightening a limb, or the position assumed by such a

                          limb

External Rotation   - Rotation away from the body.

Flexion   - The act of bending a limb, or the position assumed by such a limb

Fossa   - An anatomic depression

Humerus   - Bone of the upper arm forming the shoulder and elbow

Interosseous Membrane – A fibrous structure between the radius and ulna

Internal Rotation   - Rotation towards the body

Intramedullary Canal - Marrow cavity of a bone

IOM   - Interosseous membrane

Lateral   - Away from the middle of the body

Laxity   - Looseness

LCL   - Lateral collateral ligament; ligament composed of the LUCL and

                          the RCL

Lesser Sigmoid Notch - Depression on the lateral side of the coronoid which articulate with the radial head

Ligament   - Fibrous connective tissue between two bones

LUCL   - Lateral ulnar collateral ligament; extends from lateral epicondyle to the coronoid and serves as an important posterolateral rotational stabilizer

Medial   - Towards the middle of the body

Metacarpals   - the five bones in the hand between the wrist and the fingers

MCL   - Medial collateral ligament; extends from medial epicondyle of humerus to the coronoid providing primary valgus restraint

Morphology   - Study of size, shape and structure

NIST   - National Institute of Standards and Technology

ORIF   - Open reduction and internal fixation; method for surgically repairing fracure bone using plates and/or screws

Osseous   - Relating to bone

Osteotomy   - A surgical division or sectioning of bone

Physiologic   - In accordance with or characteristic of the normal functioning of a living organism

Posterior   - Towards the back of the body

POC   - Proximal oblique cord

Pronation   - Rotation towards the midline

Prosthesis   - Artificial device extension replacing a missing body part

Proximal   - Towards the center of the body

PRUJ   - Proximal radioulnar joint, articulation between the lesser sigmoid notch of the ulna and the circumference of the radial head

Radial Dish   - Concavity on the proximal end of the radial head which articulates with the capitellum

Radial Head   - Complex anatomic structure forming the proximal end of the radial which articulates with both the humerus and ulna

RHA   - Radial head arthroplasty

Radial Neck   - Narrow region of proxmal radius distal to the radial head

Radius   - The lateral bone of the forearm

RCL   - Radial collateral ligament; originates on the lateral epicondyle and inserts into the annular ligament serving as a primary varus stabilizer of the elbow

Sagittal   - Any vertical plane that divides the body into left and right sides

SDA   - Screw displacement axis

Soft-Tissue   - Tissues that connect, support or surround other structures, not including bone

Subluxate   - To partially dislocate a joint

Supination   - Rotation away from the midline

Trochlea   - An anatomic structure that resembles a pulley at the end of the humerus

Trochoginglymoid   - Type of joint composed of hinge (ginglymus) and pivot joints (trochoid)

Ulna   - The medial bone of the forearm articulating with the radius, humerus, and carpal bones

Curriculum Vitae

Name: Brent Lanting, FRCSC, MD, BESc

Post-secondary   The University of Western Ontario
Education and   London, Ontario, Canada
Degrees: 1998-2006 BESc, MD

                   The University of Western Ontario
                   London, Ontario, Canada
                   2006-2011 Residency – LHSC/SJHC

                   OrthoCarolina - Hip and Knee Center
                   Charlotte, North Carolina, USA
                   2011-2012 Adult Reconstruction Fellowship

Honours and   Young Investigators Initiative Grant Mentoring Program
Awards: United States Bone and Joint Initiative,   2013

                   Surgery Clerkship Resident Teaching Award,
                   Division of Orthopaedic Surgery,
                   University of Western Ontario,
                   London, Ontario, Canada   2011

                   NSERC Scholarship
                   Age hardening kinetics of Aluminum
                   University of Western Ontario
                   London, Ontario, Canada   2002

Related Work   Teaching Assistant
Experience   The University of Western Ontario
                   1993-1995

Grants:
Internal Research Grant Competition

- Evaluation of Stress levels in Surgical Trainees – A Pilot Study ($13,000)
- Dr. Howard and Milne   2013

Internal Research Grant Competition

- The Impact of Total Knee Arthroplasty Surgical Technique on Coronal Plane Motion and PatelloFemoral Articulation ($20,000)
- Dr. Howard and Teeter   2013

Physicians' Services Incorporated Foundation Resident Research Grant

- Development and Application of a Forearm Testing Apparatus ($20,000)
- Dr. King and Johnson   2007-2009

Publications:
Lanting BA, MacDonald SJ. The painful total hip replacement: diagnosis and deliverance. Bone Joint Journal. 2013 Nov;95-B(11 Suppl A):70-3

Lanting BA, Ferreira LM, Johnson JA, King GJ, Athwal GS. The Effect of Radial Head Implant Length on Radiocapitellar Articular Properties and Load Transfer within the Forearm. Journal of Orthopaedic Trauma. 2013 Oct 1.

Lanting BA, Ferreira LM, Johnson JA, Athwal GS, King GJ. The effect of excision of the radial head and metallic radial head replacement on the tension in the interosseous membrane. Bone Joint Journal. 2013 Oct;95-B(10):1383-7.

Lanting BA. Anterior Approach for Primary THR is worthwhile. Canadian Orthopaedic Association, 2013 Spring Edition, Coauthor.

Lanting B, Springer B. Catastrophic Wear in Total Hip Arthroplasty. Complete Wear-Through of a Metal-Backed Acetabular Component. Orthopaedic Clinics of North America. 2012; 43: 63-65.

Lanting B, Howard J. Peripheral Nerve Blocks in Lower Extremity Orthopaedic Surgery. Canadian Orthopaedics Association Bulletin, Spring 2012

Lanting B, Snider M, Chess D. Effect of Polyethylene Component Thickness on Range of Motion and Stability in Primary Total Knee Arthroplasty. Orthopaedics, Feb 2012.

Lanting B, McCalden R, Naudie D. Dislocated Polyethylene Inserts in Fixed-Bearing Total Knee Arthroplasty. Journal of Arthroplasty 26(2): 339, 2011.

Chinchalkar S, Lanting B, Ross D. Swan Neck Deformity after Distal Interphalangeal Joint Flexion Contractures: A Biomechanical Analysis. Journal of Hand Therapy 23(4): 420, 2010.

Lanting B, MacDermid J, Drosdowech D, Faber K. Proximal Humeral Fractures: A Systematic Review of Treatment Modalities. Journal of Shoulder and Elbow Surgery 17(1): 42, 2008.

Lanting B, Athwal G, Naudie D. Spontaneous Clostridium Perfringens Myonecrosis of the Shoulder: A Case Report. Clinical Orthopaedics and Related Research 461: 20, 2007.

Lanting B, Barfett J. Encapsulated Calcium Carbonate Suspensions: A Drug Delivery Vehicle Sensitive To Ultrasound Disruption. McGill Journal of Medicine 9: 108, 2006.

National / International Presentations:

Canadian Arthroplasty Society 2nd Annual Meeting, Montreal, QB   2013
> Podium Presentation
> Irrigation and Debridement vs Two Stage Revision: Effect on Patient
> Outcomes and Satisfaction

Canadian Orthopaedic Association 68th Annual Meeting, Win., MB   2013
> Podium Presentation
> The Effect of Radial Head Excision and Arthroplasty on Interosseous
> Membrane Loads under Dynamic Loading Conditions

Canadian Orthopaedic Association 68th Annual Meeting, Win., MB   2013
> Poster Presentation
> Simultaneous Bilateral Total Hip Artrhoplasty via the Direct Anterior
> Approach: A Safe Procedure

Canadian Orthopaedic Association 68th Annual Meeting, Win., MB   2013
> Poster Presentation
> Metal-on-Metal Hip Artrhoplasty: A Novel Technique Predicting Edge Loading
> and Subsequent Metallosis

Canadian Arthroplasty Society 1st Annual Meeting, London, ON   2012
> Podium Presentation
> Cup Position: The Effect of Approach and Intra-Operative Imaging

Canadian Orthopaedic Association 66st Annual Meeting, St. John's NL   2011
Poster Presentation
    Radial Head Prosthesis Sizing Alters the Forces in the Interosseous Membrane and
    Forearm Load Transfer

Musculoskeletal Infection Society, San Diego CA   2009
Podium Presentation
    Pseudallescheria boydii Total Knee Arthroplasty Infection: A Case Report,
    Treatment and Review of Literature

American Academy of Orthopaedic Surgeons, Las Vagas AZ   2009
Podium Presentation
    Long Term Follow-up of Medial Unicompartmental Miller-Galante Knee
    Arthroplasty

Canadian Orthopaedic Association 63rd Annual Meeting, Montreal ON   2008
Podium Presentation
    Fifteen-year Follow-up of the Miller-Galante Unicompartmental Knee Arthroplasty

Musculoskeletal Infection Society, Lake Tahoe CA   2006
Podium Presentation
    Spontaneous Clostridium Perfringens Myonecrosis of the Shoulder: A Case Report

Canadian Orthopaedic Association 61st Annual Meeting, Toronto ON   2006
Poster Presentation
    Proximal Humerus Fractures: A Systematic Review of Treatment Modalities

Book Chapters:
Published

O'Connor PJ, Lanting BA, MacDonald SJ:. Metal-on-Metal Bearings; 2013.
    Philadelphia, Saunders.

In Press

Lanting B. Use of cemented stem in revision TKA. In:Rossi R, Bonasia DE, editor(s).
    Total knee revision: Surgical techniques. 2: Minerva Medica; 2012.

Submitted

Lanting B. Removal of the Femoral and Tibial Components for revision total knee
    arthroplasty. Edizioni Minerva Medica S.p.A.; 2012.